Unifying framework for quantum simulation algorithms for time-dependent Hamiltonian dynamics

Yu Cao [1,2,3] Shi Jin [1,2,3] and Nana Liu [1,2,3,4,*]

[1]School of Mathematical Sciences, Shanghai Jiao Tong University, Shanghai 200240, China
[2]Institute of Natural Sciences, Shanghai Jiao Tong University, Shanghai 200240, China
[3]Ministry of Education Key Laboratory in Scientific and Engineering Computing, Shanghai Jiao Tong University, Shanghai 200240, China
[4]Global College, Shanghai Jiao Tong University, Shanghai 200240, China

(Received 1 April 2025; accepted 16 October 2025; published 19 November 2025)

Recently, there has been growing interest in simulating time-dependent Hamiltonians using quantum algorithms, driven by diverse applications, such as quantum adiabatic computing. While techniques for simulating time-independent Hamiltonian dynamics are well established, time-dependent Hamiltonian dynamics is less explored and it is unclear how to systematically organize existing methods and to find new methods. Sambe-Howland's continuous clock elegantly transforms time-dependent Hamiltonian dynamics into time-independent Hamiltonian dynamics, which means that by taking different discretizations, existing methods for time-independent Hamiltonian dynamics can be exploited for time-dependent dynamics. In this work, we systemically investigate how Sambe-Howland's clock can serve as a unifying framework for simulating time-dependent Hamiltonian dynamics. First, we demonstrate the versatility of this approach by showcasing its compatibility with analog quantum computing and digital quantum computing. Second, for digital quantum computers, we illustrate how this framework, combined with time-independent methods (e.g., product formulas, multiproduct formulas, qDrift, and linear combination of unitaries-Taylor), can facilitate the development of efficient algorithms for simulating time-dependent dynamics. This framework allows us to (1) resolve the problem of finding minimum-gate time-dependent product formulas; (2) establish a unified picture of both Suzuki's and Huyghebaert and De Raedt's approaches; (3) generalize Huyghebaert and De Raedt's first- and second-order formula to arbitrary orders; (4) answer an unsolved question in establishing time-dependent multiproduct formulas; (5) and recover continuous qDrift on the same footing as time-independent qDrift. Third, we demonstrate the efficacy of our higher-order Huyghebaert and De Raedt's algorithm through digital adiabatic simulation.

DOI: 10.1103/fkh5-b669

I. INTRODUCTION

The concept of quantum computers, which aim to surpass the fundamental limits of classical computers, was proposed by Feynman in 1982 [1]. Since then, this direction has attracted significant attention. As quantum computers are designed using the principles of quantum mechanics, and closed quantum systems inherently follow Schrödinger's equation (i.e., Hamiltonian dynamics with unitary evolution), the problem of simulating Hamiltonian dynamics has emerged as a core challenge across multiple disciplines. The pioneering work of Lloyd [2] introduced a foundational approach of developing quantum algorithms to simulate Hamiltonian dynamics in physics, and this study has inspired research on Hamiltonian simulation using quantum devices over the past three decades. To date, numerous quantum and quantum-classical algorithms have been proposed for simulating time-independent Hamiltonian dynamics. These include, but are not limited to, product formulas (such as the Lie-Trotter-Suzuki formula and its variants) [3–6], multiproduct formulas (MPFs) [7–10], randomized algorithms [11–14], Taylor's series [15] with linear combination of unitaries (LCU) [8], qubitization, and quantum signal processing [16]. Furthermore, detailed methods or analysis have been adapted for various situations, such as multiscale Hamiltonians [17,18] and unbounded Hamiltonians [19].

In contrast, time-dependent Hamiltonian simulation has received relatively less attention. There are several notable classical approaches. One prominent example is the time-dependent product formula developed by Huyghebaert and De Raedt [20] and contemporaneously by Suzuki [21]. Another popular approach is the Magnus-based method [22], which often requires combination with product formulas or LCU to be implemented on quantum hardware. Recently, researchers have, for instance, explored time-dependent multiproduct formula [23], time-dependent qubitization [23–25], and time-dependent qDrift [26], as well as time-dependent algorithm with minimum gate counts [27]. However, it appears that there is a lack of a systematic approach to leverage the benefits and advances in recent studies on time-independent Hamiltonian simulation problems for time-dependent situations within the community. Several questions raised by some of these works remain partially addressed, leaving open questions or only provide limited solutions for special instances.

*Contact author: nana.liu@quantumlah.org

Published by the American Physical Society under the terms of the Creative Commons Attribution 4.0 International license. Further distribution of this work must maintain attribution to the author(s) and the published article's title, journal citation, and DOI.

This motivates us to provide a *systemic way* through Sambe-Howland's clock to (1) recover many existing time-dependent algorithms using time-independent algorithms; (2) establish the connection between some popular algorithms in literatures; (3) provide the mathematical machinery of using Sambe-Howland's clock; (4) and more importantly, to develop high-order Huyghebaert and De Raedt's algorithm, which was discussed as an open question in a recent work [27].

To the best of our knowledge, Sambe-Howland clock, an elegant and powerful tool, appears to have been underappreciated for time-dependent Hamiltonian simulation algorithms. We also observe that technical challenges arise for discrete variants of Sambe-Howland's clock in designing quantum algorithms. Since it seamlessly connects time-dependent Hamiltonian dynamics with time-independent Hamiltonian dynamics, it allows us to use the richer set of tools from the latter to find algorithms for the former case. Thus, this motivates us to investigate how the *continuous form* of Sambe-Howland's clock can be exploited as a unifying framework from which existing time-dependent Hamilton simulation algorithms can be derived, and also to enhance existing algorithms by applying existing methods for time-independent Hamiltonian dynamics to time-dependent Hamiltonian dynamics.

A. Problem setup

To properly setup the problem, our goal is to simulate the following time-dependent Schrödinger's equation:

$$\partial_t|\psi(t)\rangle = -iH(t)|\psi(t)\rangle, \quad t \in [0,1].$$

Such equations might arise from many scenarios, e.g., digitized adiabatic simulation [28], dynamics in the interaction picture [29], or from the resulting equation after applying Schrödingerization [30–33] for quantum simulation of general linear ordinary differential equations (ODEs) and partial differential equations (PDEs). The time-evolution operator for $s \leqslant t$ is defined as follows:

$$\mathcal{U}(t,s) := \exp_{\mathcal{T}}\left(-i\int_s^t H(r)\,\mathrm{d}r\right). \tag{1}$$

The notation $\mathcal{T}$ is the time-chronological ordering operator. The ordering of the noncommutative Hamiltonian is conceived as an inconvenience in simulating the time-dependent Schrödinger's equation in a digital quantum circuit. As a result, this has been a very active research topic in recent years to address this issue.

Assumption 1. We consider Hamiltonians with the following form:

$$H(t) = \sum_{k=1}^{\Lambda} H_k(t). \tag{2}$$

This structure has received much attention and has been used in numerous studies. We assume that $H_k(t)$ are smooth with respect to the time variable. The time domain $\mathbb{T}$ can be either a one-dimensional (1D) torus or simply $\mathbb{R}$. All operators $H_k(t)$ are defined on a finite-dimensional Hilbert space $\mathcal{H}$.

For instance, one may consider that

$$H_k(t) = f_k(t)\boldsymbol{h}_k, \quad f_k \in C^\infty(\mathbb{T}), \tag{3}$$

and $\boldsymbol{h}_k$ are operators on a finite-dimensional Hilbert space $\mathcal{H}$ with bounded norm. Though most algorithms discussed below only rely on the form in Eq. (2) and the regularity assumption above, we remark that the choice of Eq. (3) is also not very restrictive, e.g., for studying digitized adiabatic simulation. The Hamiltonian $H(t)$ with the form in Eq. (3) belongs to the linear combination (LC) model. When we further assume that $\boldsymbol{h}_k$ are unitary, this becomes the linear combination of unitary model. Notably, it is well established that the LC model also encompasses the sparse Hamiltonian case, as shown in, e.g., Refs. [26,34].

B. Sambe-Howland's clock

The Sambe-Howland's clock Hamiltonian introduces a conjugate pair of the time variable (commonly referred to as the energy in physical literature) into the original time-dependent Hamiltonian, effectively transforming a time-dependent Schrödinger's equation into a time-independent one [35,36]. This formalism is also known as the (t,t') method in the literature [37] and has been applied to various situations, including steady-state perturbation theory [35], scattering theory [36], open quantum system [38], quantum computing [23] (where a discrete version was employed), and simulation of time-dependent PDEs using analog quantum computing [33]. The Sambe-Howland's clock Hamiltonian proceeds as follows [35–37,39]: by augmenting the quantum dynamics with a continuous auxiliary state s and defining the Sambe-Howland's clock Hamiltonian:

$$\overline{H} = \hat{p}_s \otimes \mathbf{I} + H(\hat{s}). \tag{4}$$

Here, the s mode—with corresponding quadrature operators $\hat{s}$ and $\hat{p}_s$ where $[\hat{s},\hat{p}_s] = i\mathbf{I}_s$—is referred to as the clock mode.

With the extended Hamiltonian $\overline{H}$, one can evolve the closed Hamiltonian dynamics in the extended space:

$$\begin{aligned}\partial_t|\Psi(t)\rangle &= -i\overline{H}|\Psi(t)\rangle,\\ |\Psi(0)\rangle &= \left(\int G(s)|s\rangle\right)\otimes|\psi(0)\rangle,\end{aligned} \tag{5}$$

which amounts to solving the following PDE (see, e.g., Ref. [39, Chapter X.12] and also Refs. [33,35–37]):

$$\begin{aligned}\partial_t\Psi(t,s,\cdot) &= -\partial_s\Psi(t,s,\cdot) - iH(s)\Psi(t,s,\cdot),\\ \Psi(0,s,\cdot) &= G(s)\psi(0).\end{aligned} \tag{6}$$

As the first term $-\partial_s\Psi(t,s,\cdot)$ plays the role as the transport, one can directly use the method of characteristics and verify that the exact solution takes the form [36, Theorem 1]

$$|\Psi(t)\rangle = \int \mathrm{d}s\, G(s-t)|s\rangle\otimes\mathcal{U}(s,s-t)|\psi(0)\rangle. \tag{7}$$

Remark 1. This expression has tight connection to LCU, as it has the form of an infinite linear combination (namely, the integration) of unitary evolution with fixed time span t and with various terminal time s.

Note that the state G could be totally artificial (namely, introduced merely for the mathematical purpose), if we only use this formalism as an intermediate step to derive some algorithms. If the state G needs to be physical (e.g., used for analog quantum computing), a common choice of G is to use

TABLE I. This table summarizes how various choices of ω and how different discretizations of the clock mode connect to different quantum algorithms. We colored our results and focus in red. The limit $\omega \to 0$ means it is a localized state and $\omega \to \infty$ is used to denote that $G \equiv 1$.

	Hamiltonian (digital)	**Hamiltonian (analog)**
clock (analog)	hybrid system	**fully analog** (see Section III) $\omega = \mathcal{O}\left(\frac{1}{T\|\boldsymbol{h}_2\|}\right)$
clock (digital)	**fully digital** (see below)	hybrid system

ω	**Discretize s mode**	**Algorithms**	**Relevant Sections**
limit $\omega \to 0$ (G is a delta measure) or limit $\omega \to \infty$ ($G = 1$)	operator splitting	product formula and its variants (e.g., multi-product formula, randomized product formula)	Section IV, Section V, Section VI, Section VII
limit $\omega \to 0$ (G is a delta measure) or limit $\omega \to \infty$ ($G = 1$)	Taylor's expansion	LCU-Taylor based algorithm	Section VIII
when $0 < \omega \ll 1$	finite difference	qubitization-based method; so far limited to the first-order [23]	/
limit $\omega \to \infty$ ($G = 1$)	spectral method	qubitization-based method; log scale wrt error tolerance ϵ under conditions [24, 25]	/

the Gaussian state where

$$G(s) = \frac{1}{(2\pi\omega^2)^{1/4}} e^{-\frac{s^2}{4\omega^2}}. \tag{8}$$

This formalism is different from the Feynman's clock, which encodes the full-history Hamiltonian simulation problem into the ground state problem [40], whereas Sambe-Howland's clock only worries about preparing the quantum state at a particular time. We summarize possible variants as well as our focus in this paper in Table I.

C. Related works for time-dependent Hamiltonian simulation

In this subsection, we will provide an overview of existing methods for time-independent Hamiltonian simulations, with a particular focus on related works that explore quantum algorithms for time-dependent Hamiltonian dynamics. The following *nonexhaustive discussion* will introduce and examine methods that may be adaptable to the Sambe-Howland's clock, as well as the Magnus expansion as a parallel framework. Readers may refer to, e.g., Ref. [41] for a review and additional discussions.

Product formulas: The product formula is arguably the most extensively studied family of quantum algorithms for Hamiltonian simulation [3–6,20,42], also known as the Lie-Trotter-Suzuki formula. In the time-independent case, this approach has been analyzed, e.g., in Ref. [34] and more recently, the error estimate has been meticulously studied in Ref. [43]. This family of schemes boasts benefits from commutator scaling [43], a feature that many scaling-optimal algorithms (to be discussed later) may not possess. Regarding time-dependent Hamiltonian simulations, Huyghebaert and De Raedt generalized the Strang-splitting scheme (a second-order scheme) to the time-dependent case [20] in 1990s. Concurrently, Suzuki proposed a general framework for deriving time-dependent Hamiltonian simulation algorithms up to any order using low-order product formulas [21,44]. A detailed error analysis for Suzuki's scheme [21] was further developed in Ref. [45] and adaptive schemes have been explored in, e.g., Refs. [46,47] to enhance efficacy for practical considerations.

Multiproduct formulas: For product-based formulas, the way to achieve arbitrary high-order algorithm is to use a large number of iterative passes of local Hamiltonian evolution operator (namely, the multiplicative construction). The multiproduct formula instead uses the idea of Richardson's extrapolation (namely, additive construction) and the time-independent case was studied in, e.g., Refs. [7–10,48]. For the time-dependent case, Geiser combined product-based formulas with extrapolation techniques [49] to develop multiproduct formulas. A different variant was recently posted as an open technical question in Ref. [23] for well-conditioned multiproduct formula. Notably, when combined with LCU techniques, multiproduct formulas are known to achieve logarithmic error scaling [9,48], whereas the error scaling for product-based formulas is always suboptimal and algebraic.

Randomized algorithm: Various randomization ideas have been found to be practical and useful in quantum algorithms for Hamiltonian simulation. Examples include randomizing the ordering in product formulas [12,13], randomizing the time step [11,12], and randomly selecting local unitary evolutions in a full sequence (known as the "qDrift algorithm") [14]. In particular, the latter idea has attracted much

attention recently, and has been generalized to stochastic Hamiltonian sparsification [50], partially random algorithm [51,52], qSWIFT (a high-order generalization of qDrift) [53], cost-informed choice for the importance weight [54], and others. As for time-dependent Hamiltonian simulation, a time-dependent analog of qDrift, also known as the "continuous qDrift," was proposed in Ref. [26]. Although this scheme is insightful, there appears to be a lack of deeper structural connection between the time-dependent case and time-independent case, which we will discuss and address later.

Taylor's series method and Dyson's series method. Taylor's expansion for time-independent Hamiltonian simulation algorithm in LCU form was initially studied in Ref. [15], which demonstrated that the complexity scales logarithmically with respect to the error precision $\mathcal{O}\big(T\frac{\log(T/\epsilon)}{\log\log(T/\epsilon)}\big)$ and this scaling cannot be achieved using product formulas with finite orders. As a remark, for the 1D Heisenberg model, it has been demonstrated in Ref. [55] that Taylor's series method is not competitive empirically, compared with both product formula and quantum signal processing. The time-dependent generalization of Taylor series method was developed in Refs. [29,56] using Dyson's expansion, further improved in Ref. [26] to obtain L^1 norm scaling estimate, and also studied in Ref. [57] using permutation expansion.

Quantum signal processing/Qubitization. The qubitization technique for time-independent Hamiltonian simulation has been shown to achieve optimal complexity scaling, matching the theoretical lower bound [16]. This technique utilized the Jacobi-Anger expansion, differing from other related works that employ Taylor's type expansions [15]. The initial study on its time-dependent generalization was presented in Ref. [23], which is limited to a first-order algorithm. Another approach has been presented recently in Ref. [24] for the case where time schedules are periodic (also known as the Sambe's space). A further generalization to multi-periodic time-dependent Hamiltonians has been explored in Ref. [25]. For time-periodic Hamiltonians, their query complexity in Ref. [24] matches the optimal one provided by time-independent qubitization. This result has also demonstrated, from a different perspective, the value of Sambe-Howland's formalism in designing quantum algorithms at least for periodic case. Consequently, Sambe-Howland's clock for quantum algorithms warrants a more systematic study and presentation.

Magnus expansion. Magnus expansion has been a widely studied tool for time-dependent dynamics [22], as well as Hamiltonian simulation problems recently, as seen in works such as Refs. [17,18,27,58–62]. Typically, after performing a finite truncation of the Magnus expansion, it is necessary to additionally employ a quadrature scheme to estimate the integration if required, and then apply Hamiltonian simulation techniques like product formulas [17,18,27,60–62], or LCU and quantum signal processing (see below) [58,59]. A key challenge in applying the Magnus expansion to quantum algorithms is the need to implement nested commutators. The community has proposed at least two approaches to address this issue. One is to use the commutator-free quasi-Magnus (CFQM) operators [62–64]. As remarked above, while the CFQM method effectively handles time dependence, it requires additional Hamiltonian simulation algorithms, such as product formulas, to be used in conjunction with it. Another commutator-free approach involves leveraging Magnus-based ideas to directly develop asymmetric product formulas, as demonstrated in Refs. [27,61]. We remark that Magnus's expansion is a parallel framework in the same way as Sambe-Howland's clock, and it would be interesting to see whether there is any chance to further unify them.

D. Summary of results

We take Sambe-Howland's clock as our starting point, and systemically investigate how to leverage the advances in time-independent Hamiltonian simulation problems to tackle the time-dependent case.

Various computational models. We will demonstrate that this framework can be applied to analog quantum computing with detailed analysis on how to choose ω. The primary focus of this work is to develop algorithms suitable for digital quantum computers, which we will elaborate on in details below.

Product formula. As mentioned above, there are two main approaches for directly handing time dependence, Huyghebaert and De Raedt's approach (which utilizes the access to time integration of local Hamiltonians) and Suzuki's approach (which utilizes access to pointwise local Hamiltonians). Specifically, Huyghebaert and De Raedt approached the time-dependent problem by drawing on insights and natural generalizations; Suzuki introduced his renowned time operator to address the problem of time ordering. These two parallel approaches can be, in fact, unified within the framework of Sambe-Howland's clock, which offers a straightforward way to design product formulas for time-dependent case. In fact, Suzuki had briefly commented on the possibility of Sambe-Howland's clock approach in Ref. [21, Sec. 6]; unfortunately, it seems that this path has not yet been seriously explored so far.

(1) In this work, we show that Sambe-Howland's clock approach provides a unified framework that can lead to both Huyghebaert and De Raedt's and Suzuki's approaches, just via different decomposition of $\overline{H}$ in Eq. (4).

(2) By applying time-independent scheme directly to Sambe-Howland's clock and with appropriate decomposition, we generalize Huyghebaert and De Raedt's approach to arbitrary high order, which was discussed still as an unknown problem in recent literatures [27].

(3) This approach also enables us to, from a different perspective, resolve the problem of finding quantum algorithms for time-dependent problems with minimum number of gates, as studied recently in Ref. [27].

(4) Since we need to introduce an unbounded operator $\hat{p}_s = -i\partial_s$ into a perhaps bounded Hamiltonian $H(s)$, it brings a concern about its mathematical soundness when G in Eq. (8) is chosen as a delta measure. This concern actually can be straightforwardly answered by choosing $G \equiv 1$ and using Sambe-Howland's clock as an intermediate step rather than as an actual quantum protocol.

The top panel of Table II gives a visual summary of our main results, and see Secs. IV and V for technical details. As a remark, we only list the case $\Lambda = 2$ for simplicity of

TABLE II. This table summarizes how Sambe-Howland's clock (with $\omega \to 0$) can be used as a mathematical tool to uncover existing quantum algorithms and also unravel quantum algorithms for time-dependent Hamiltonian simulation. For the ordered decomposition, we only list the case where the number of local Hamiltonian is $\Lambda = 2$ for simplicity; "Gate (general)" means the number of gates for one-step approximation without any assumption on original Hamiltonian, whereas "Gate (DAS)" means the number of gates for digital adiabatic simulation where $H_k(s) = f_k(s)\boldsymbol{h}_k$. We assume that time-independent decomposition has q cycles as in Eq. (21) below.

Sambe-Howland's clock with product formula $\overline{H} = A_1 + A_2 + A_3$

Ordered decomposition	Time-independent	Time-dependent	Gate (general)	Gate (DAS)
$A_1 = \hat{p}_s \otimes \mathbf{I}$ $A_2 = H_1(\hat{s})$ $A_3 = H_2(\hat{s})$	[6] Any product formula with q cycles	[21] Theorem 6	$2\Lambda q - q$ $2\Lambda q - q$	$2\Lambda q - 2q + 1$ $2\Lambda q - 2q + 1$
$A_1 = H_1(\hat{s})$ $A_2 = \hat{p}_s \otimes \mathbf{I}$ $A_3 = H_2(\hat{s})$	Any product formula with q cycles	Theorem 6	$2\Lambda q - 2q + 1$	$2\Lambda q - 2q + 1$
$A_1 = \hat{p}_s \otimes \mathbf{I} + H_1(\hat{s})$ $A_2 = -\hat{p}_s \otimes \mathbf{I}$ $A_3 = \hat{p}_s \otimes \mathbf{I} + H_2(\hat{s})$	First-order Trotter Strang splitting ($q = 1$)	[20] [20]	Λ $2\Lambda - 1$	Λ $2\Lambda - 1$
	Any product formula with q cycles	Theorem 8	$2\Lambda q - 2q + 1$	$2\Lambda q - 2q + 1$

Sambe-Howland's clock with multiproduct formula $\overline{H} = A_1 + A_2 + A_3$

Ordered decomposition	Base	Time-independent MPF	Time-dependent MPF
$A_1 = \hat{p}_s \otimes \mathbf{I}$ $A_2 = H_1(\hat{s})$ $A_3 = H_2(\hat{s})$	Strang splitting	[9]	Theorem 9 (using continuous clock) (Conjectured in Ref. [23] using discrete clock) (cf. Ref. [49] using Suzuki's time operator)
$A_1 = \hat{p}_s \otimes \mathbf{I} + H_1(\hat{s})$ $A_2 = -\hat{p}_s \otimes \mathbf{I}$ $A_3 = \hat{p}_s \otimes \mathbf{I} + H_2(\hat{s})$			see Theorem 10

Sambe-Howland's clock with qDrift $\overline{H} = \sum_{k=1}^{\Lambda} \int_0^1 \mathrm{d}r\, \mu(k,r)(\hat{p}_s \otimes \mathbf{I} + \frac{H_k(\hat{s})}{\mu(k,r)})$, where μ is any probability measure for $(k, r) \in \{1, 2, \ldots, \Lambda\} \times [0, 1]$

Measures	Time-independent qDrift	Time-dependent qDrift	Error scaling	Notes
$\mu(k, r) = \mu_k$ is independent of r	[14]	see Eq. (35)	see Lemma 12	–
General measure μ		see Eq. (37)	see Lemma 13	recover "continuous qDrift" [26]; see Lemma 14

illustration, but main results are stated for a general $\Lambda \in \mathbb{N}$ later; the decomposition order of $\overline{H}$ in the table matters as these operators are noncommutative.

Multiproduct formula. MPF for time-dependent case was recently studied in Ref. [23]; however, one important component is only stated as a conjecture, which we will explore using the continuous Sambe-Howland's clock. Due to the tight connection between Suzuki's formula and Huyghebaert and De Raedt's approach within the framework of Sambe-Howland's clock, we can immediately replace the base formula in MPF to Huyghebaert and De Raedt's second-order algorithm, and similarly to other higher-order base schemes. The middle panel of Table II gives a visual summary.

Randomized algorithm. We also investigate the resulting formula by applying the time-independent qDrift into the Sambe-Howland's clock formalism, and under suitable decompositions, we can recover the continuous qDrift proposed by Ref. [26]. The benefit of Sambe-Howland's formalism enables us to analyze, e.g., the bias from time-dependent qDrift almost in the same way as time-independent qDrift. This is summarized in the bottom panel of Table II.

Finite-order LCU-Taylor algorithm. We also explore how Taylor's expansion may be directly applied to Sambe-Howland's clock to derive quantum algorithms with finite order. Specifically, we will show how to directly derive a second-order LCU-Taylor algorithm using Sambe-Howland's clock, as a possible alternative candidate to Dyson's expansion. Its generalization to other finite-order algorithms is straightforward and is not pursued herein. Although these algorithms do not achieve optimal scaling, they are relatively easier for understanding and have straightforward implementation. Moreover, such algorithms serve as a testament to the versatility of Sambe-Howland's clock in providing a systematic approach to developing quantum algorithms.

Numerical experiments. We perform numerical experiments on our high-order Huyghebaert and De Raedt's

algorithm. Leveraging recent advances in optimizing time-independent product formulas (see, e.g., Refs. [65,66]), we can seamlessly extend these improvements to the time-dependent case, yielding more practically efficient product formulas for time-dependent simulations. We consider four different fourth-order decompositions summarized in Ref. [66] for demonstration and compare with a Magnus-motivated product formula [27] equipped with the same time-independent scheme. This family of algorithms exhibits better performance for digitized adiabatic simulation. We remark that wider benchmark experiments are surely needed for further validation, but these experiments have already showcased how Sambe-Howland's clock can assist with the design of efficient quantum algorithms.

Remark. We acknowledge a related contemporary independent work [67], which employs Floquet theory to derive explicit error bounds for time-dependent product formulas and multiproduct formulas. While there is a thematic connection between our work (particularly Secs. V and VI) and Ref. [67], we emphasize that the technical approaches are distinct. Unlike Ref. [67], our approach does not need to rely on the periodic embedding of time-dependent Hamiltonians. Instead, we present a more general and flexible methodology applicable to product formulas utilizing both pointwise-query and integral-based query models, as well as other types of quantum algorithms. On the contrary, Ref. [67] provided an error bound with commutator scaling, a result not yet pursued in this paper. Consequently, while both studies draw inspiration from the Sambe-Howland's clock formalism, they are complementary, differing in their primary findings and focuses, as well as technical details.

E. Notations

We denote the Hilbert space of the original Hamiltonian simulation problem as $\mathcal{H}$. Suppose A_k are operators for $k = 1, 2, \ldots, \Lambda$, where Λ is an arbitrary positive integer, then

$$\prod_{k=1}^{\Lambda} e^{A_k} := e^{A_1} e^{A_2} \cdots e^{A_\Lambda}, \quad \prod_{k=\Lambda}^{1} e^{A_k} := e^{A_\Lambda} \cdots e^{A_2} e^{A_1}.$$

As operators are generally noncommutative, these two notations are distinct. We denote $|\mathbb{1}\rangle$ as the constant function with value one in the domain $\mathbb{T}$ for the s mode. We remark that this state $|\mathbb{1}\rangle$ could be un-normalized, which is introduced merely for mathematical purposes. For any operator A on a Hilbert space $\mathcal{H}$, the notation $\|A\|_p$ means the Schatten-p norm for $p \in [1, \infty]$; for any superoperator $\mathcal{A}$, the notation $\|\mathcal{A}\|_p$ means the induced p norm acting on the density matrices of $\mathcal{H}$, namely, $\|\mathcal{A}\|_p := \sup_\rho \|\mathcal{A}(\rho)\|_p$, where the supremum is taken over all possible density matrices ρ. The notation $\mathcal{U}(t, s)$ denotes the target time-dependent unitary evolution; $U(t)$ denotes the time-independent unitary evolution; $U(t, s)$ denotes the time-dependent unitary evolution (used for approximation),; $\widetilde{U}(t, s)$ denotes the Huyghebaert and De Raedt's unitary evolution (used for approximation); and $e_{\mathcal{T}} \equiv \exp_{\mathcal{T}}$ denotes the time-ordered exponential.

II. PRELIMINARIES: COMPUTATIONAL MODELS, APPLICATIONS, AND MORE ON SAMBE-HOWLAND'S CLOCK

A. Computational models

Sambe-Howland's clock provides a generic approach to transform a time-dependent problem into time-independent one. However, depending on how one chooses the localized state G [namely, ω in Eq. (8)] and whether one intends to use auxiliary G as a true physical ancilla mode or merely an artificial one purely for mathematical purposes, one could develop different quantum algorithms suitable for various quantum architecture starting from Sambe-Howland's clock.

1. The idealized case ($\omega \to 0$)

For the idealized case where one chooses the Dirac delta function (as a mathematical tool only), there are two equivalent ways to recover the original state:

(1) *(Localized version)*. If the auxiliary state $G = \delta(\cdot - t)$ is the Dirac delta function centered at t and $Q \equiv 1$, then

$$\langle Q|\langle\varphi|e^{-i\overline{H}t'}|G\rangle|\psi\rangle = \langle\varphi|\mathcal{U}(t + t', t)|\psi\rangle. \tag{9}$$

It means one can prepare a localized state, and then trace out all the auxiliary degree of freedom to recover the desired state $\mathcal{U}(t + t', t)|\psi\rangle$.

(2) *(Delocalized version)*. If the auxiliary state $G \equiv 1$ and Q is the Dirac delta function centered at $t + t'$, then

$$\begin{aligned}(\langle G|\langle\psi|e^{i\overline{H}t'}|Q\rangle|\varphi\rangle)^* &= \langle Q|\langle\varphi|e^{-i\overline{H}t'}|G\rangle|\psi\rangle \\ &= \langle\varphi|\mathcal{U}(t + t', t)|\psi\rangle.\end{aligned} \tag{10}$$

In later applications, we will typically choose $t' = \Delta t$ to be small to develop product formulas for one time step. It can be observed that these two versions (9) and (10) are essentially the *conjugate pair* to each other.

2. For analog quantum computing ($\omega > 0$)

For analog quantum computing where one can only perform measurement rather than direct integration, it is easy to show that for the full dynamics (5) on the augmented space

$$\begin{aligned}\rho_\omega(t) &:= \mathrm{tr}_s(|\Psi(t)\rangle\langle\Psi(t)|) \\ &= \int \mathrm{d}s |G(s - t)|^2 \mathcal{U}(s, s - t)|\psi(0)\rangle\langle\psi(0)|\mathcal{U}(s, s - t)^\dagger.\end{aligned} \tag{11}$$

Again, when G is localized at 0, then

$$\mathrm{tr}_s(|\Psi(t)\rangle\langle\Psi(t)|) \approx \mathcal{U}(t, 0)|\psi(0)\rangle\langle\psi(0)|\mathcal{U}(t, 0)^\dagger.$$

As was remarked in Ref. [33], one does not necessarily need to prepare the auxiliary state G as a pure state. Due to the linearity in the auxiliary state, it can be a mixed state whose diagonal components are localized at zero. For simplicity, we shall stick with the pure state formalism. Experimentally, one could approximately prepare a squeezed Gaussian state $|G\rangle$ with variance $\mathcal{O}(\omega^2)$ as in Eq. (8).

B. Digitized adiabatic simulation

Given two Hamiltonians $\boldsymbol{h}_1$ and $\boldsymbol{h}_2$, together with a schedule $f : [0, 1] \to [0, 1]$ satisfying $f(0) = 0$ and $f(1) = 1$, and the timescale T, one can control a wave function to slowly move from the ground state of $\boldsymbol{h}_1$ to the ground state of $\boldsymbol{h}_2$ [28]:

$$\begin{aligned} \partial_t|\psi(t)\rangle &= -iH(t)|\psi(t)\rangle, \\ H(t) &= H_1(t) + H_2(t), \\ H_1(t) &= f_1(t)\boldsymbol{h}_1, \quad f_1(t) = T(1 - f(t)), \\ H_2(t) &= f_2(t)\boldsymbol{h}_2, \quad f_2(t) = Tf(t). \end{aligned} \tag{12}$$

The initial state $|\psi(0)\rangle$ is chosen as the ground state of $\boldsymbol{h}_1$. Typically, one takes the time $T \gg 1$ to ensure accuracy. The choices of optimal schedule f and T are important to achieve high efficiency. In this work, as our goal is to simulate time-dependent Hamiltonians rather than optimizing its schedule path, we assume that these choices are already made.

Assumption 2. Let us denote the exact ground state of $\boldsymbol{h}_2$ as $|\varphi_{\text{true}}\rangle$. Assume that the time T and the schedule f have been chosen such that

$$|\langle\psi(1)|\varphi_{\text{true}}\rangle - 1| = \mathcal{O}(\epsilon) \tag{13}$$

or equivalently

$$\||\psi(1)\rangle\langle\psi(1)| - |\varphi\rangle\langle\varphi|\|_{\text{tr}} = \mathcal{O}(\sqrt{\epsilon}). \tag{14}$$

This assumption means that in follow-up applications, we will not optimize the schedule nor time span T as in, e.g., Refs. [68,69], but rather only focus on simulating such a dynamics using quantum architecture.

C. The functional space of Sambe-Howland's clock

When one considers the digitized adiabatic simulation, one could always restrict the time domain to [0, 1]; therefore, one can always find a smooth extension of this Hamiltonian simulation problem to a torus with periodic boundary conditions on H_k. In case one considers unbounded time domain, one may simply choose $\mathbb{T} = \mathbb{R}$. In what follows, we shall only consider these two situations. For the augmented Hamiltonian dynamics (5), we consider the following functional space:

$$\mathscr{X} := \{f \in C^\infty(\mathbb{T}; \mathbb{C}) : \|f^{(m)}\|_{L^\infty(\mathbb{T})} < \infty\} \otimes \mathcal{H},$$

where $f^{(m)}$ means the mth order derivative of f. For problems with lower regularity conditions, one could possibly resolve the regularity issues e.g., by first approximating the problem with smooth enough Hamiltonians. Dealing with such technicalities is beyond the scope of this work, and we shall exclusively focus on smooth functions throughout this work. Thus, the above functional space $\mathscr{X}$ is sufficient and natural to work on.

D. Sambe-Howland's clock and the perspective of numerical PDEs

In what follows, we shall elaborate on the details in Table I from the numerical PDE's perspective. Recall that Sambe-Howland's clock essentially transforms the time-dependent Hamiltonian dynamics into a PDE. In particular, the first term in the augmented Hamiltonian $\hat{p}_s \otimes \mathbf{I}$ contributes as a transport term. For instance, when $H(s) = -\frac{1}{2M}\partial_{xx} + f(s)V(x)$ is a time-dependent particle Hamiltonian under the potential V and with particle mass M, the above construction transforms an s-dependent elliptic-type operator $H(s)$ into a parabolic type for $\overline{H}$, and the Schrödinger's equation on the augmented space is

$$\begin{aligned} \partial_t\Psi(t, s, x) = -\partial_s\Psi(t, s, x) + \frac{i}{2M}\partial_{xx}\Psi(t, s, x) \\ + (-i)f(s)V(x)\Psi(t, s, x). \end{aligned}$$

As one is dealing with PDEs, the most natural approaches to consider are finite difference method, spectral method, and operator splitting. Of course, the finite-element method is also possible to consider and it might be useful for developing other types of quantum algorithms; however, we will not consider it for the time being. First, we will discuss a challenge of using finite-difference method and discuss why we should consider the limiting situation $\omega \to 0$ or $\omega \to \infty$ for digital quantum computers. As for spectral methods and operator-splitting methods, we will discuss their advantages and limitations; the first one was studied in Refs. [24,25] for periodic Hamiltonians, and we will study operator-splitting methods later as well as many variants.

Finite-difference method for $0 < \omega \ll 1$. When we use a Gaussian state with small but nonzero ω as an approximate in Eq. (8), then the most natural approach is the finite-difference method. A challenge (also mentioned in Ref. [23]) is that as the momentum operator has very large norm $\mathcal{O}(\frac{1}{\Delta s})$ after discretization (where Δs is the mesh size in the s mode), it appears to be difficult to go beyond the first-order algorithm in terms of gate complexity, even using theoretically optimal algorithm like qubitization.

Spectral method for $\omega \to \infty$. In Refs. [24,25], the spectral method was employed using the Fourier basis with periodic boundary condition. One can discretize the s variable using the Fourier basis and project the whole dynamics into a finite number of basis functions. This approach is beneficial if the error of spectral method for the Hamiltonian dynamics (5) decays exponentially fast with respect to the number of basis functions chosen. This is the case when $H(t)$ is sufficiently smooth. As discussed above, choosing such a Fourier basis will very likely necessitate the projection into a localized state (namely using the delocalized version), and therefore, the amplitude amplification methods are necessary and perhaps unavoidable as were used in Ref. [24]. This suggests that quantum algorithms built upon this approach are unlikely to be implementable without the fault-tolerance quantum computer.

Operator-splitting methods as ω *approaches 0 or* ∞. To develop practical algorithms from the Sambe-Howland's formalism, another natural way is to develop product-based formula (namely, operator splitting) for such a formalism. It turns out that for both $\omega = 0$ and ∞, one will end up with the same final time-dependent product formula. The case $\omega = 0$ is more physically intuitive in terms of the derivation as the s mode in this case aligns better with the "time" variable, whereas the case $\omega = \infty$ can more easily provide mathemat-

ical convenience. However, we remark that both formalisms are technically equivalent.

Summary. From the above nonexhaustive discussion, it appears that to make the Sambe-Howland's clock formalism suitable for digital quantum platform in practice, it might be desirable that we choose $\omega \to 0$ and $\omega \to \infty$ in order to avoid the order restriction, and also choose operator splitting or many variants to avoid the possible implementation challenge. This leads into Secs. IV–VII below.

III. ANALOG QUANTUM COMPUTING

When the Hamiltonian itself is inherently defined for qumodes (namely, continuous-variable quantum state), the most straightforward way is to adopt analog quantum computing [32,33,70] to realize the Hamiltonian simulation. In Ref. [33], the continuous form of the Sambe-Howland model was used to turn nonautonomous linear PDEs into time-independent Hamiltonian dynamics that can be simulated on an analog quantum device. In this section, we will first review this formalism and discuss how to achieve high-order approximation with respect to the Gaussian width $\omega > 0$ for general problems. For digitized adiabatic simulation, as the computational model is fully analog, we will also discuss how to pick ω for the squeezed Gaussian state.

A. High-order approximation via Richardson's extrapolation

Recall that the Sambe-Howland's clock Hamiltonian is given as $\overline{H} = \hat{p}_s \otimes \mathbb{I} + H(\hat{s})$. One evolves the closed Hamiltonian dynamics

$$\partial_t \sigma(t) = -i[\overline{H}, \sigma(t)],$$
$$\sigma(0) = \rho_0 \otimes |\psi(0)\rangle\langle\psi(0)|, \quad \rho_0 = |G\rangle\langle G|,$$

where G is chosen as the squeezed Gaussian state (8). It has been shown in Ref. [33] that if $\omega \ll 1$, one has

$$\| |\psi(t)\rangle\langle\psi(t)| - \rho_\omega(t) \|_{\mathrm{tr}} \leqslant \sqrt{C}\omega,$$

where C is some constant. This estimate yields a first-order algorithm. The scaling of ω can be improved via, e.g., Richardson's extrapolation if one mainly focuses on the estimates of an observable $\widehat{O}$ on $\mathcal{H}$. This technique has been used for error mitigation [10] and multiproduct formulas [7–9] for Hamiltonian simulation.

Theorem 3. Recall ρ_ω from Eq. (11) and suppose G is given in Eq. (8). For any observable $\widehat{O}$ with $\|\widehat{O}\|_\infty \leqslant 1$, and suppose coefficients $\{\alpha_j\}_{j=1}^M \subseteq \mathbb{R}$ and integer-valued time steps $\{k_j\}_{j=1}^M \subseteq \mathbb{N}$ are well chosen to satisfy

$$\begin{bmatrix} 1 & 1 & \cdots & 1 \\ k_1^{-2} & k_2^{-2} & \cdots & k_M^{-2} \\ \vdots & \vdots & \vdots & \vdots \\ k_1^{-2(m-1)} & k_2^{-2(m-1)} & \cdots & k_M^{-2(m-1)} \end{bmatrix} \begin{bmatrix} \alpha_1 \\ \alpha_2 \\ \vdots \\ \alpha_M \end{bmatrix} = \begin{bmatrix} 1 \\ 0 \\ \vdots \\ 0 \end{bmatrix}. \tag{15}$$

Then,

$$\left| \sum_{j=1}^M \alpha_j \mathrm{tr}\big(\widehat{O}\rho_{\omega/k_j}(t)\big) - \langle\psi(t)|\widehat{O}|\psi(t)\rangle \right| \leqslant 2\sqrt{C_m}\omega^m + \mathcal{O}(\omega^{m+2}),$$

where C_m is a constant whose expression can be found in Eq. (A1).

The proof is postponed to Appendix A 1.

B. Gaussian width estimate for digitized adiabatic simulation

Next, we will specialize the above error estimation for digitized adiabatic simulation. For digitized adiabatic simulation problem in Eq. (12), the Hamiltonian takes the following more specific form:

$$\overline{H} = \hat{p}_s \otimes \mathbb{I} + f_1(\hat{s}) \otimes \boldsymbol{h}_1 + f_2(\hat{s}) \otimes \boldsymbol{h}_2. \tag{16}$$

Under Assumption 2, the adiabatic path gives the error scaling $\mathcal{O}(\sqrt{\epsilon})$ in trace norm in Eq. (13). In the following, we provide an estimate of the choice of ω in order to maintain the same scaling of error.

Theorem 4 (Choice of ω for fully analog digitized adiabatic simulation). Suppose that $\epsilon \ll 1$ and $\omega \ll 1$. By further imposing the constraint

$$\omega = \mathcal{O}\left(\frac{1}{T\|\boldsymbol{h}_2\|}\right), \tag{17}$$

then one can ensure that

$$\|\mathrm{tr}_s(|\Psi(t)\rangle\langle\Psi(t)|) - |\varphi_{\mathrm{true}}\rangle\langle\varphi_{\mathrm{true}}|\|_{\mathrm{tr}} = \mathcal{O}(\sqrt{\epsilon}), \tag{18}$$

which has the same asymptotic error scaling as digitized adiabatic simulation formalism (13).

The proof is postponed to Appendix A 2. We remark that the scaling of T (implicitly) depends on the precision ϵ, and the precise dependence is determined by the digitized adiabatic simulation problem itself and the schedule f chosen.

Remark 2. This formalism is beneficial if $\|\boldsymbol{h}_2\| = \mathcal{O}(1)$ as in the case of the adiabatic Grover's search algorithm; see Sec. IX A below. The above scaling also linearly depends on T^{-1}, which is very likely to be optimal, as the Hamiltonian in the augmented system $\|\overline{H}\| = \mathcal{O}(T)$.

IV. PRODUCT FORMULA (I): POINTWISE QUERY TO $\boldsymbol{H_k(s)}$

Product formula is arguably the most widely studied and practical algorithm in Hamiltonian simulation, and we will first discuss how Sambe-Howland's clock can be used to develop time-dependent product formulas. This perspective could date back to a comment in Sec. 6 of Suzuki's celebrated work [21], but as far as we know, it has not been formally adopted and studied in detail in the literature. Suzuki's $\overleftarrow{\partial}/\partial t$ operator in Ref. [21] is not rigorously specified in his original work, and Sambe-Howland's clock Hamiltonian precisely provides the right mathematical object.

We will first illustrate the idea of Sambe-Howland's clock for simple examples in Sec. IV A for first-order and second-order cases, and then generalize this idea to arbitrary high-order algorithms in Sec. IV B, given any time-independent product formula. Then, we will demonstrate

and discuss in Sec. IV C that using this approach, the time-dependent product formulas could only use the same number of gates as the corresponding time-independent counterparts. In particular, this suggests a route to design a time-dependent scheme with minimum number of gates for arbitrary high order, which generalizes Ref. [27]. We will explain its connection with Suzuki's formalism in Sec. IV D. Concerning the mathematical rigorousness, we shall comment on why Sambe-Howland's clock offers the right tool in Sec. IV E without the need to deal with Gaussian approximation of delta measure as was probably needed in discrete clock analog [23].

A. Illustrative examples: first order and second order

We begin with heuristic explanation on how Sambe-Howland's clock enables one to develop product formulas for time-dependent Hamiltonian simulation. The augmented Hamiltonian takes the following form:

$$\overline{H} = \hat{p}_s \otimes \mathbf{I} + \sum_{k=1}^{\Lambda} H_k(\hat{s}).$$

This operator is time-independent, and one can apply the following Lie's formula (first-order product formula), $e^{-i\Delta t\overline{H}} \approx e^{-i\Delta t \hat{p}_s \otimes \mathbf{I}} \prod_{k=1}^{\Lambda} e^{-i\Delta t H_k(\hat{s})} + \mathcal{O}(\Delta t^2)$. Therefore,

$$\begin{aligned} & e^{-i\Delta t\overline{H}}|t\rangle \otimes |\psi(t)\rangle \\ & \approx e^{-i\Delta t\ \hat{p}_s\otimes \mathbf{I}} \prod_{k=1}^{\Lambda} e^{-i\Delta t H_k(\hat{s})}|t\rangle \otimes |\psi(t)\rangle + \mathcal{O}(\Delta t^2) \\ & \approx e^{-i\Delta t\ \hat{p}_s}\ |t\rangle\ \otimes \prod_{k=1}^{\Lambda} e^{-i\Delta t H_k(t)}|\psi(t)\rangle + \mathcal{O}(\Delta t^2) \\ & = |t+\Delta t\rangle \otimes \prod_{k=1}^{\Lambda} e^{-i\Delta t H_k(t)}|\psi(t)\rangle. \end{aligned}$$

By the time-localized version (9), one knows that $\langle \mathbb{1}|_s e^{-i\Delta t\overline{H}}|t\rangle \otimes |\psi(t)\rangle = \mathcal{U}(t+\Delta t, t)|\psi(t)\rangle$. This implies that one can approximate the time-dependent Hamiltonian evolution via

$$\mathcal{U}(t+\Delta t, t) \approx \prod_{k=1}^{\Lambda} e^{-i\Delta t H_k(t)} + \mathcal{O}(\Delta t^2).$$

To get this, we have used the fact that $\langle \mathbb{1}||t+\Delta t\rangle \equiv \int_{\mathbb{T}} 1 \cdot \delta(s-(t+\Delta t))\,\mathrm{d}s = 1$. This formula is essentially the analog of Euler's method for ODEs. If we apply the Strang-splitting scheme (namely, a second-order Trotter, or also known as the midpoint scheme), then similarly,

$$\begin{aligned} & \langle \mathbb{1}|_s e^{-i\Delta t\overline{H}}|t\rangle \otimes |\psi(t)\rangle \\ & \approx \langle \mathbb{1}|_s e^{-i\hat{p}_s\otimes \mathbf{I}\Delta t/2} \prod_{k=1}^{\Lambda} e^{-i\frac{\Delta t}{2}H_k(\hat{s})} \prod_{k=\Lambda}^{1} \\ & \quad \times\ e^{-i\frac{\Delta t}{2}H_k(\hat{s})} e^{-i\hat{p}_s\otimes \mathbf{I}\ \Delta t/2}|t\rangle \otimes |\psi(t)\rangle \\ & = \prod_{k=1}^{\Lambda} e^{-i\frac{\Delta t}{2}H_k(t+\Delta t/2)} \prod_{k=\Lambda}^{1} e^{-i\frac{\Delta t}{2}H_k(t+\Delta t/2)}|\psi(t)\rangle. \end{aligned}$$

This suggests the following approximation:

$$\mathcal{U}(t+\Delta t, t) \approx \prod_{k=1}^{\Lambda} e^{-i\frac{\Delta t}{2}H_k(t+\Delta t/2)} \prod_{k=\Lambda}^{1} e^{-i\frac{\Delta t}{2}H_k(t+\Delta t/2)}. \quad (19)$$

This scheme is also known as the second-order Trotter for the time-dependent Hamiltonian, and in some literature, it is known as the midpoint scheme. This scheme also has the minimum number of operator exponentials when $\Lambda = 2$ for the second-order product formulas; see, e.g., Ref. [27]. When the Hamiltonian is time-independent, one recovers the midpoint scheme for time-independent Hamiltonians:

$$e^{-iH\Delta t} \approx \prod_{k=1}^{\Lambda} e^{-i\frac{\Delta t}{2}H_k} \prod_{k=\Lambda}^{1} e^{-i\frac{\Delta t}{2}H_k}. \quad (20)$$

B. A general scheme

In a recent work, Ostmeyer [66] proved that a product formula for two local operators with order n can yield a general scheme with the same order for Λ local operators. The conclusion was stated for time-independent operator splitting methods.

Theorem 5 ([66, Theorem 1]). Suppose there is a product formula with order n such that for arbitrary two operators A and B,

$$e^{(A+B)\Delta t} = e^{Aa_1\Delta t}e^{Bb_1\Delta t}\cdots e^{Bb_q\Delta t}e^{Aa_{q+1}\Delta t} + \mathcal{O}(\Delta t^{n+1}), \quad (21)$$

then for any $\Lambda \geqslant 1$ and a collection of operators $\{A_k\}_{k=1}^{\Lambda}$,

$$\begin{aligned} e^{\Delta t\sum_{k=1}^{\Lambda}A_k + \mathcal{O}(\Delta t^{n+1})} = & \left(\prod_{k=1}^{\Lambda} e^{A_k c_1 \Delta t}\right)\left(\prod_{k=\Lambda}^{1} e^{A_k d_1 \Delta t}\right)\cdots \\ & \left(\prod_{k=1}^{\Lambda} e^{A_k c_q \Delta t}\right)\left(\prod_{k=\Lambda}^{1} e^{A_k d_q \Delta t}\right), \end{aligned} \quad (22)$$

where

$$\begin{aligned} & c_1 = a_1, \quad c_k = a_k - d_{k-1}, \quad k = 2,\ldots,q, \\ & d_k = b_k - c_k, \quad k = 1,2,\ldots,q. \end{aligned}$$

In what follows, we generalize such a result to the time-dependent case, without increasing the number of operator exponentials in the product formula and without affecting the order of convergence.

Theorem 6. Suppose that the time-independent Hamiltonian can be decomposed as in Eq. (2). Under the same assumption of Theorem 5, the following scheme gives an order n approximation of the time-ordered unitary evolution $\mathcal{U}(t+\Delta t, t) \equiv \exp_{\mathcal{T}}(-i\int_t^{t+\Delta t} H(s)\,\mathrm{d}s)$:

$$\begin{aligned} U_n(t+\Delta t, t) := & U_F(t+L_1, t+R_1)U_B(t+R_1, t+L_2)\cdots \\ & U_F(t+L_{q-1}, t+R_{q-1})U_B(t+R_{q-1}, t+L_q) \\ & U_F(t+L_q, t+R_q)U_B(t+R_q, t+0), \end{aligned} \quad (23)$$

TABLE III. This table lists the number of (local) gates for time-dependent schemes for various Λ'. In this estimate, we consider the most general form, and there is no need to assume $\hat{H}_k(s)$ to be commutative in time (namely, the above estimate is valid even if $[H_k(s), H_k(t)] \neq 0$ for $s \neq t$). When we consider the digitized adiabatic simulation, the number of gates is *always* $2\Lambda q - (2q-1)$ for any such time-dependent schemes, no matter how to choose Λ'.

Method	Parameter	Number of gates
Time-independent case	n/a	$\boldsymbol{2\Lambda q - (2q-1)}$
Time-dependent case	$\Lambda' \neq 0$ and $\Lambda' \neq \Lambda$	$\boldsymbol{2\Lambda q - (2q-1)}$
	$\Lambda' = 0$	$2\Lambda q - q$
	$\Lambda' = \Lambda$	$2\Lambda q - (q-1)$

where

$$U_F(t',t) = \prod_{k=1}^{\Lambda'} e^{-i(t'-t)H_k(t')} \prod_{k=\Lambda'+1}^{\Lambda} e^{-i(t'-t)H_k(t)},$$
$$U_B(t',t) = \prod_{k=\Lambda}^{\Lambda'+1} e^{-i(t'-t)H_k(t')} \prod_{k=\Lambda'}^{1} e^{-i(t'-t)H_k(t)},$$

and $\Lambda' \in \{0, 1, 2, \ldots, \Lambda\}$ is arbitrary, with the coefficients satisfying the following relations: for $k = 1, 2, \ldots, q$,

$$L_k = \Delta t \sum_{j=k}^{q} (c_j + d_j), \quad L_{q+1} \equiv 0,$$
$$R_k = \Delta t \left(d_k + \sum_{j=k+1}^{q} (c_j + d_j) \right).$$

Suppose one is given query access to matrix exponentials of the form $e^{-i\Delta t H_k(\alpha)}$ for any index k, time α, and time step Δt. The resources needed are summarized in Table III.

Proof. We first present a proof based on the localized version (9) to illustrate the ideas. A second proof that is more friendly for mathematical rigorousness will be given in later subsections. For the augmented Hamiltonian, we can choose

$$\begin{aligned} A_k &= -iH_k(\hat{s}), \quad k \leqslant \Lambda', \\ A_{\Lambda'+1} &= -i\hat{p}_s \otimes \mathbf{I}, \\ A_k &= -iH_{k-1}(\hat{s}), \quad k > \Lambda'+1. \end{aligned} \tag{24}$$

Then, by the localized version (9) and by Eq. (21),

$$\begin{aligned} & U(t+\Delta t, t)|\psi\rangle \\ & \overset{(9)}{=} \langle \mathbb{1}|_s e^{-i\Delta t \overline{H}} |t\rangle \otimes |\psi\rangle \\ & \overset{(21)}{=} \langle \mathbb{1}|_s \left(\prod_{k=1}^{\Lambda+1} e^{A_k c_1 \Delta t} \right) \left(\prod_{k=\Lambda+1}^{1} e^{A_k d_1 \Delta t} \right) \cdots \\ & \left(\prod_{k=1}^{\Lambda+1} e^{A_k c_q \Delta t} \right) \left(\prod_{k=\Lambda+1}^{1} e^{A_k d_q \Delta t} \right) |t\rangle \otimes |\psi\rangle + \mathcal{O}(\Delta t^{n+1}). \end{aligned}$$

For instance, one can easily verify that

$$\begin{aligned} & \prod_{k=\Lambda+1}^{1} e^{A_k d_q \Delta t} |t\rangle \otimes |\psi\rangle \\ & = \prod_{k=\Lambda+1}^{\Lambda'+2} e^{A_k d_q \Delta t} e^{A_{\Lambda'+1} \Delta t} \prod_{k=\Lambda'}^{1} e^{A_k d_q \Delta t} |t\rangle \otimes |\psi\rangle \\ & = \prod_{k=\Lambda+1}^{\Lambda'+2} e^{A_k d_q \Delta t} e^{A_{\Lambda'+1} \Delta t} \left(|t\rangle \otimes \prod_{k=\Lambda'}^{1} e^{-iH_k(t) d_q \Delta t} |\psi\rangle \right) \\ & = \prod_{k=\Lambda+1}^{\Lambda'+2} e^{A_k d_q \Delta t} \left(|t + d_q \Delta t\rangle \otimes \prod_{k=\Lambda'}^{1} e^{-iH_k(t) d_q \Delta t} |\psi\rangle \right) \\ & = |t + d_q \Delta t\rangle \otimes U_B(t + d_q \Delta t, t) |\psi\rangle. \end{aligned}$$

Consequently, after applying all previous $2q-1$ terms and finally applying $\langle \mathbb{1}|_s$, we can straightforwardly verify the formula (23).

After going through all multiplicative construction of operator exponential, there seems to be $2\Lambda q$ gates in Eq. (23). In fact, one can remove some overcounted gates from H_1 and H_Λ; e.g., one can merge operators with the form $e^{-ic_1 H_\Lambda(t)} e^{-id_1 H_\Lambda(t)}$ into a single operator exponential $e^{-i(c_1+d_1)H_\Lambda(t)}$.

(1) When $\Lambda' = 0$, the gate corresponding to H_Λ are overcounted but the gates for H_1 cannot be combined, which leads into the estimate $2\Lambda q - (q-1)$. This can be more explicitly seen by the following: consider

$$\begin{aligned} & U_F(t + L_k, t + R_k) U_B(t + R_k, t + L_{k+1}) \\ & \quad = \prod_{k=1}^{\Lambda} e^{-i(L_k - R_k)H_k(t+R_k)} \prod_{k=\Lambda}^{1} e^{-i(R_k - L_{k+1})H_k(t+R_k)}, \end{aligned}$$

and therefore, the gate for H_Λ is overcounted; however, one cannot merge gates for H_1 if $H_1(t + R_k)$ does not commute with $H_1(t + R_{k+1})$ for the following:

$$\begin{aligned} & U_B(t + R_k, t + L_{k+1}) U_F(t + L_{k+1}, t + R_{k+1}) \\ & \quad = \prod_{k=\Lambda}^{1} e^{-i(R_k - L_{k+1})H_k(t+R_k)} \prod_{k=1}^{\Lambda} e^{-i(L_{k+1} - R_{k+1})H_k(t+R_{k+1})}. \end{aligned}$$

Overall, for the most general case, the number of gates is $2\Lambda q - q$, whereas for digitized adiabatic simulation, one only needs $2\Lambda q - (2q-1)$ gates.

(2) When $\Lambda' \neq 0$ and $\Lambda' \neq \Lambda$, at each junction of U_F and U_B operators, we can similarly verify that there is one overcounted gate, and this leads into the estimate $2\Lambda q - (2q-1)$.

(3) When $\Lambda' = \Lambda$, the gate estimate is similar to the above cases.

■

C. Discussion on the minimum-gate implementation

The above Theorem 6 suggests that as long as we pick $\Lambda' \neq 0, \Lambda$, then the time-dependent product formula above always uses the same number of gates as the time-independent product formula under a very general condition. Suppose that we already have a time-independent product formula with the minimum number of gates for a certain fixed order (where the

order can be arbitrary), then the time-dependent formula given by Theorem 6 must also achieve the minimal number of gates. This generalizes the result in Ref. [27]. Moreover, their algorithm in Ref. [27] is not directly applicable for Hamiltonians with more than two local terms; a similar algorithm is only stated in the context of qubit systems in Ref. [61] (though not aiming at achieving the minimal number of gates). The above scheme (23), however, is capable of handing a general Λ.

For example, for fourth-order product formulas, the Forest-Ruth-Suzuki (FRS) formula [5,66,71] achieves the minimum number of gates:

$$e^{X+Y} \approx e^{\frac{\gamma}{2}X} e^{\gamma Y} e^{\frac{1-\gamma}{2}X} e^{(1-2\gamma)Y} e^{\frac{1-\gamma}{2}X} e^{\gamma Y} e^{\frac{\gamma}{2}X}, \tag{25}$$

where $\gamma = (2 - 2^{1/3})^{-1} \approx 1.351\,207$. This product formula has the minimum number of gates for two local operators, which makes it suitable for digitized adiabatic simulation. Reference [27] used this formula to derive a product formula for time-dependent Hamiltonian simulation based on Magnus expansion and it admits the following form:

$$\begin{aligned}
&\mathcal{T} e^{-i\int_t^{t+\Delta t} H_1(s)+H_2(s)\,\mathrm{d}s} \\
&\quad \approx e^{-i(\frac{\gamma\beta_1}{2}+u)H_1} e^{-i\gamma\beta_2 H_2} e^{-i\frac{1-\gamma}{2}\beta_1 H_1} e^{-i(1-2\gamma)\beta_2 H_2} \\
&\qquad \times e^{-i\frac{1-\gamma}{2}\beta_1 H_1} e^{-i\gamma\beta_2 H_2} e^{-i(\frac{\gamma\beta_1}{2}-u)H_1},
\end{aligned} \tag{26}$$

where

$$\begin{aligned}
\beta_1 &= \int_t^{t+\Delta t} f_1(s)\mathrm{d}s, \\
\beta_2 &= \int_t^{t+\Delta t} f_2(s)\mathrm{d}s, \\
u &= \frac{1}{2\beta_2}\int_t^{t+\Delta t} \mathrm{d}s_1 \int_t^{s_1} \mathrm{d}s_2\, f_1(s_1)f_2(s_2) - f_2(s_1)f_1(s_2).
\end{aligned}$$

By Eq. (23) and when $\Lambda' = 1$, the time-dependent product formula is

$$\begin{aligned}
&\mathcal{T} e^{-i\int_t^{t+\Delta t} H_1(s)+H_2(s)\,\mathrm{d}s} \\
&\quad \approx e^{-i\frac{\gamma\Delta t}{2}\hat{H}_1(t+\Delta t)} e^{-i\gamma\Delta t\hat{H}_2(t+(1-\frac{\gamma}{2})\Delta t)} \\
&\qquad \times e^{-i\frac{(1-\gamma)\Delta t}{2}\hat{H}_1(t+(1-\gamma)\Delta t)} e^{-i(1-2\gamma)\Delta t\hat{H}_2(t+\frac{\Delta t}{2})} \\
&\qquad \times e^{-i\frac{(1-\gamma)\Delta t}{2}\hat{H}_1(t+\gamma\Delta t)} e^{-i\gamma\Delta t\hat{H}_2(t+\frac{\gamma\Delta t}{2})} e^{-i\frac{\gamma\Delta t}{2}\hat{H}_1(t)}.
\end{aligned} \tag{27}$$

This formula has the same number of gates compared with Eq. (26) derived from Ref. [27], which means it also has the minimum possible gates for a time-dependent Hamiltonian simulation problem.

D. Connection to Suzuki's approach

In what follows, we shall discuss how the above scheme (23) connects to Suzuki's original approach and a few potential advantages of the approach that we take here.

Recovery of Suzuki's formula. When one takes $\Lambda' = 0$ and considers the case $c_j = d_j$ for $1 \leqslant j \leqslant q$, one knows that for the cycle j in Eq. (23), one has $L_j - R_j = c_j\Delta t = d_j\Delta t = R_j - L_{j+1}$, and the building block in Eq. (23) for the jth cycle:

$$\begin{aligned}
&U_F(t+L_j, t+R_j)U_B(t+R_j, t+L_{j+1}) \\
&\quad = \prod_{k=1}^{\Lambda} e^{-ic_k\Delta t H_k(t+R_j)} \prod_{k=\Lambda}^{1} e^{-id_k\Delta t H_k(t+R_j)}
\end{aligned}$$

is essentially the midpoint scheme in Eq. (24) in Ref. [21], or Eq. (9) in Ref. [45] (an analytical work for Suzuki's time-dependent scheme), and the final overall scheme is basically the time-dependent formula by Suzuki.

Possible advantage of Sambe-Howland's clock. This approach is mathematically similar to Suzuki's approach whereas the approach from Sambe-Howland's clock offers a perspective to view Suzuki's time operator with a more explicit mathematical structure, as well as possible physical interpretations. More specifically, (1) it avoids the necessity to handle or justify the operator $\overleftarrow{\partial}/\partial t$ [21] whose mathematical justification is not well discussed; if we view Suzuki's approach in the language of Sambe-Howland's clock, the functional space is more clear as explained in Sec. II C and Suzuki's time operator is essentially the momentum operator acting on the augmented space. (2) Sambe-Howland's clock Hamiltonian provides a physical interpretation for Suzuki's formulas, and in particular, $\overleftarrow{\partial}/\partial t$ can be exactly interpreted as the extra auxiliary state as a "clock." We acknowledge that his original operator exactly plays the role as a physical clock but it may not be as explicitly stated as Sambe-Howland's clock.

E. On the mathematical concerns and the second proof

1. Discussion on the mathematical concern

The above derivation of product formulas uses the transport equation of a delta measure $|t\rangle = \delta(s-t)$, which is mathematically well defined for the space of generalized distributions. However, a reasonable concern is that the operator $\hat{p}_s$ is not well defined when acting on a delta measure $|t\rangle$, which leads into a concern that when we estimate the error or perform Taylor's expansion of $e^{-i\hat{p}_s\Delta t} = \sum_{k=0}^{\infty} (-i\hat{p}_s\Delta t)^k/k!$, the series is not well defined when acting on $|t\rangle|\psi\rangle$ where $|\psi\rangle \in \mathcal{H}$. This perspective was discussed for the discrete clock case recently in Ref. [23, Sec. IV]. However, the delocalized formalism in Eq. (10), the conjugate formalism of the localized one, can exactly avoid this concern.

The reason is the following: for a smooth function $|\Psi\rangle \in \mathscr{X}$, $\hat{p}_s \otimes \mathbf{I}$ is surely well defined acting on $|\Psi\rangle$ and thus the translation operator $e^{-i\Delta t\hat{p}_s\otimes\mathbf{I}}$ is also well defined; the inner product $\langle t+\Delta t|_s|\Psi\rangle \equiv \Psi(t+\Delta t, \cdot)$ is also bounded for $|\Psi\rangle \in \mathscr{X}$, and we do not need to interpret $\langle t+\Delta t|$ as a delta measure but equivalently as retrieving the function value of a smooth function on the augmented space. Therefore, it becomes clear that the delocalized version could be made mathematically rigorous as long as the input state $|\Psi\rangle$ is smooth with respect to the s variable.

In what follows, we will provide a second proof of Theorem 6, showing that the delocalized formalism (10) gives the same approximation (and thus automatically the same

error term) as the localized formalism (9). This suggests that both approaches, the localized version (9) and the delocalized version (10), could be made mathematically rigorous with appropriate interpretations.

2. The second proof of Theorem 6

Let us consider the delocalized version (10). Before getting into the detailed proofs, we shall list some facts in Lemma 7, whose proof is postponed to Appendix A 3.

Lemma 7. If one adopts the same notation as in Eq. (24), then for any s', $\theta \in \mathbb{R}$, $|\varphi\rangle \in \mathcal{H}$, and any $|\Psi\rangle \in \mathscr{X}$, one has

$$\langle s'|\langle\varphi|\prod_{k=1}^{\Lambda+1} e^{A_k\theta\Delta t}|\Psi\rangle = \langle s'-\theta\Delta t|\langle\varphi|(\mathbf{I}\otimes U_F(s',s'-\theta\Delta t))|\Psi\rangle$$

and

$$\langle s'|\langle\varphi|\prod_{k=\Lambda+1}^{1} e^{A_k\theta\Delta t}|\Psi\rangle = \langle s'-\theta\Delta t|\langle\varphi|(\mathbf{I}\otimes U_B(s',s'-\theta\Delta t))|\Psi\rangle.$$

Recall that the delocalized version (10) gives the following: For any $|\psi\rangle \in \mathcal{H}$,

$$\begin{aligned}
&\langle\varphi|\mathcal{U}(t+\Delta t,t)|\psi\rangle\\
&= \langle t+\Delta t|\langle\varphi|e^{-i\overline{H}\Delta t}|\mathbb{1}\rangle|\psi\rangle\\
&= \langle t+\Delta t|\langle\varphi|\left(\prod_{k=1}^{\Lambda+1} e^{A_k c_1\Delta t}\right)\left(\prod_{k=\Lambda+1}^{1} e^{A_k d_1\Delta t}\right)\cdots\left(\prod_{k=1}^{\Lambda+1} e^{A_k c_q\Delta t}\right)\left(\prod_{k=\Lambda+1}^{1} e^{A_k d_q\Delta t}\right)|\mathbb{1}\rangle|\psi\rangle + \mathcal{O}(\Delta t^{n+1})\\
&= \langle t+\Delta t-c_1\Delta t|(\langle\varphi|U_F(t+L_1,t+R_1))\left(\prod_{k=\Lambda+1}^{1} e^{A_k d_1\Delta t}\right)\cdots\left(\prod_{k=1}^{\Lambda+1} e^{A_k c_q\Delta t}\right)\left(\prod_{k=\Lambda+1}^{1} e^{A_k d_q\Delta t}\right)|\mathbb{1}\rangle|\psi\rangle + \mathcal{O}(\Delta t^{n+1})\\
&= \cdots \overset{(23)}{=} \langle t|\langle\varphi|\mathbf{I}\otimes U_n(t+\Delta t,t)|\mathbb{1}\rangle|\psi\rangle + \mathcal{O}(\Delta t^{n+1}) = \langle\varphi|U_n(t+\Delta t,t)|\psi\rangle + \mathcal{O}(\Delta t^{n+1}).
\end{aligned}$$

To get the third equality, we used the fact that $L_1 = \Delta t$ and $R_1 = \Delta t - c_1\Delta t$. This provides a second proof of Theorem 6.

Remark 3. We emphasize that the state $|\Psi\rangle \in \mathscr{X}$ in the augmented space does not need to be a physical state, and we merely use the bra-ket notation for consistency. In particular, for the case $H_k(s) = f(s)\boldsymbol{h}_k$, with appropriate assumptions on the high-order derivatives of $f \in C^\infty(\mathbb{T})$, one can expect that all operations are well defined. However, we notice that such a nice property does not seem to hold for the discretized Sambe-Howland's clock with $\omega > 0$, which leads to unsolved technicalities in Ref. [23] when they applied the firstly discretized Sambe-Howland's clock to multiproduct formulas. We will elaborate further how Sambe-Howland's clock in the *continuous form* can assist with resolving this problem in Sec. VI below.

V. PRODUCT FORMULA (II): QUERY TO THE TIME INTEGRATION OF $H_k(s)$

In this section, we will demonstrate how Sambe-Howland's clock can establish generalized schemes of Huyghebaert and De Raedt's approach [20] to arbitrary high order, by assuming queries to $\exp_{\mathcal{T}}(-i\int_t^{t+\Delta t} H_k(s)\,\mathrm{d}s)$ for any t and small Δt. Product-based formulas along this line appear to be much less studied, compared to Suzuki's operator $\overleftarrow{\partial}/\partial t$. Such a generalization seems to be unknown in the literature, to the best of our knowledge, and was also discussed as an open question in a recent work [27]. In this section, we will derive high-order Huyghebaert and De Raedt schemes (or HDR scheme in short) based on Sambe-Howland's clock, and these schemes turn out to be very efficient in handling time for digitized adiabatic simulation.

First, we will illustrate the main idea and show how Strang-splitting scheme together with appropriate decomposition of Sambe-Howland's clock Hamiltonian can recover the second-order scheme of Huyghebaert and De Raedt in Sec. V A. Then, in Sec. V B, given any time-independent product formula, we will show how to find a corresponding HDR scheme with the same order. We emphasize that such a family of high-order scheme does not increase the number of unitary gates required, which addresses the problem of finding minimum-gate implementation in Ref. [27] from yet another different perspective, besides the approach in Sec. IV C.

A. An illustrative example

When $\Lambda = 2$, a time-dependent generalization of Strang-splitting scheme (midpoint scheme) was studied in Ref. [20]:

$$\begin{aligned}
&\mathcal{U}(t+\Delta t,t)\\
&\approx e_{\mathcal{T}}^{-i\int_{t+\frac{\Delta t}{2}}^{t+\Delta t} H_1(s)\,\mathrm{d}s}\, e_{\mathcal{T}}^{-i\int_{t+\frac{\Delta t}{2}}^{t+\Delta t} H_2(s)\,\mathrm{d}s}\, e_{\mathcal{T}}^{-i\int_{t}^{t+\frac{\Delta t}{2}} H_2(s)\,\mathrm{d}s}\, e_{\mathcal{T}}^{-i\int_{t}^{t+\frac{\Delta t}{2}} H_1(s)\,\mathrm{d}s}\\
&\equiv e_{\mathcal{T}}^{-i\int_{t+\frac{\Delta t}{2}}^{t+\Delta t} H_1(s)\,\mathrm{d}s}\, e_{\mathcal{T}}^{-i\int_{t}^{t+\Delta t} H_2(s)\,\mathrm{d}s}\, e_{\mathcal{T}}^{-i\int_{t}^{t+\frac{\Delta t}{2}} H_1(s)\,\mathrm{d}s}.
\end{aligned}$$

If one considers digitized adiabatic simulation, then one simply has, e.g.,

$$e_{\mathcal{T}}^{-i\int_{t+\frac{\Delta t}{2}}^{t+\Delta t} H_1(s)\,\mathrm{d}s} = e^{-i\int_{t+\frac{\Delta t}{2}}^{t+\Delta t} H_1(s)\,\mathrm{d}s}.$$

To establish the connection between their scheme and Sambe-Howland's clock, let us divide the Hamiltonian $\overline{H}$ into

$$\overline{H} = \underbrace{(\hat{p}_s \otimes \mathbf{I} + H_1(\hat{s}))}_{=:A_1} + \underbrace{-\hat{p}_s \otimes \mathbf{I}}_{=:A_2} + \underbrace{(\hat{p}_s \otimes \mathbf{I} + H_2(\hat{s}))}_{=:A_3}$$

and apply the Strang splitting (second order) for these three (time-independent) operators:

$$\begin{aligned}
e^{-i\overline{H}\Delta t}|t\rangle|\phi\rangle &\approx e^{-iA_1\frac{\Delta t}{2}} e^{-iA_2\frac{\Delta t}{2}} e^{-iA_3\frac{\Delta t}{2}} e^{-iA_3\frac{\Delta t}{2}} e^{-iA_2\frac{\Delta t}{2}} \left(e^{-iA_1\frac{\Delta t}{2}}|t\rangle|\phi\rangle\right) \\
&\overset{(9)}{=} e^{-iA_1\frac{\Delta t}{2}} e^{-iA_2\frac{\Delta t}{2}} e^{-iA_3\frac{\Delta t}{2}} e^{-iA_3\frac{\Delta t}{2}} e^{-iA_2\frac{\Delta t}{2}} |t+\Delta t/2\rangle \left(e_{\mathcal{T}}^{-i\int_t^{t+\frac{\Delta t}{2}} H_1(s)\mathrm{d}s}|\phi\rangle\right) \\
&= e^{-iA_1\frac{\Delta t}{2}} e^{-iA_2\frac{\Delta t}{2}} e^{-iA_3\frac{\Delta t}{2}} e^{-iA_3\frac{\Delta t}{2}} |t\rangle \left(e_{\mathcal{T}}^{-i\int_t^{t+\frac{\Delta t}{2}} H_1(s)\mathrm{d}s}|\phi\rangle\right) \\
&= e^{-iA_1\frac{\Delta t}{2}} e^{-iA_2\frac{\Delta t}{2}} e^{-iA_3\frac{\Delta t}{2}} |t+\Delta t/2\rangle \left(e_{\mathcal{T}}^{-i\int_t^{t+\frac{\Delta t}{2}} H_2(s)\mathrm{d}s} e_{\mathcal{T}}^{-i\int_t^{t+\frac{\Delta t}{2}} H_1(s)\mathrm{d}s}|\phi\rangle\right) \\
&= \vdots \\
&= |t+\Delta t\rangle \otimes \left(e_{\mathcal{T}}^{-i\int_{t+\frac{\Delta t}{2}}^{t+\Delta t} H_1(s)\mathrm{d}s} e_{\mathcal{T}}^{-i\int_{t+\frac{\Delta t}{2}}^{t+\Delta t} H_2(s)\,\mathrm{d}s} e_{\mathcal{T}}^{-i\int_t^{t+\frac{\Delta t}{2}} H_2(s)\,\mathrm{d}s} e_{\mathcal{T}}^{-i\int_t^{t+\frac{\Delta t}{2}} H_1(s)\mathrm{d}s}|\phi\rangle\right).
\end{aligned}$$

This is essentially the midpoint scheme developed above after we trace out the additional degree of freedom in the s variable (or say ignore the s variable).

Unlike Suzuki's approach that uses pointwise access to $H_k(s)$, the above scheme uses the time-integrated Hamiltonian, whereas the whole derivation is essentially the same as the time-independent case. Moreover, one only needs to apply time-independent schemes in the Sambe-Howland's clock to derive both Suzuki's formula and Huyghebaert and De Raedt's second-order algorithm.

B. A general scheme

Due to the above connection of Huyghebaert and De Raedt's second-order scheme with Sambe-Howland's clock, we can derive a whole family of time-dependent high-order schemes along the line of Huyghebaert and De Raedt's approach, in a very systemic way. When given the Λ operators, we can split the Hamiltonian $\overline{H}$ via the following:

$$\begin{aligned}
\overline{H} = &\underbrace{(\hat{p}_s \otimes \mathbf{I} + H_1(\hat{s}))}_{=:A_1} + \underbrace{(-\hat{p}_s \otimes \mathbf{I})}_{=:A_2} + \underbrace{(\hat{p}_s \otimes \mathbf{I} + H_2(\hat{s}))}_{=:A_3} + \cdots \\
&+ \cdots + \underbrace{(-\hat{p}_s \otimes \mathbf{I})}_{=:A_{2\Lambda-2}} + \underbrace{(\hat{p}_s \otimes \mathbf{I} + H_\Lambda(\hat{s}))}_{=:A_{2\Lambda-1}}.
\end{aligned} \tag{28}$$

In total, there are $2\Lambda - 1$ operators. By applying any time-independent product-based formula for this, we immediately end up with the following approximation:

Theorem 8. Suppose that the time-independent Hamiltonian can be decomposed as in Eq. (2). Under the same assumption of Theorem 5, the following scheme gives an order n approximation of the time-ordered unitary evolution $\mathcal{U}(t+\Delta t, t)$:

$$\begin{aligned}
&\widetilde{U}_n(t+\Delta t, t) \\
&:= \widetilde{U}_F(t+L_1, t+R_1)\widetilde{U}_B(t+R_1, t+L_2)\cdots \\
&\quad \widetilde{U}_F(t+L_{q-1}, t+R_{q-1})\widetilde{U}_B(t+R_{q-1}, t+L_q) \\
&\quad \widetilde{U}_F(t+L_q, t+R_q)\widetilde{U}_B(t+R_q, t+0),
\end{aligned} \tag{29}$$

where

$$\widetilde{U}_F(t', t) = \prod_{k=1}^{\Lambda} e_{\mathcal{T}}^{-i\int_t^{t'} H_k(s)\mathrm{d}s},$$

$$\widetilde{U}_B(t', t) = \prod_{k=\Lambda}^{1} e_{\mathcal{T}}^{-i\int_t^{t'} H_k(s)\mathrm{d}s}.$$

Suppose we are given query access to $e_{\mathcal{T}}^{-i\int_t^{t'} H_k(s)\,\mathrm{d}s}$ for any t, t', and the index k, this generalized HDR scheme always only uses $2\Lambda q - (2q-1)$ gates for each time step, and therefore, it costs no extra gates compared with the time-independent product formula.

Proof. The proof is essentially the same as the above illustrative example except that we apply Theorem 5 for high-order splitting in place of the second-order Strang scheme. The detailed derivation is no different from Theorem 6. ■

Remark 4. When we choose the Forest-Ruth-Suzuki formula (25) in Theorem 8, the explicit expression is given in Eq. (A4). Such a scheme is different from Eq. (26) derived by Magnus's expansion in Ref. [27]. Similarly, one could derive the relevant sixth-order algorithm with minimum gate complexity by applying Yoshida's sixth-order formula, and theoretically to any order.

VI. TIME-DEPENDENT MULTIPRODUCT FORMULA

In this section, we will show how the Sambe-Howland's continuous clock formalism can help to establish the MPF used as quantum algorithms for time-dependent Hamiltonian simulation. The MPF for time-dependent cases was proposed in Ref. [23] using discretized Sambe-Howland's clock. However, one important foundational result was only proposed as a conjecture due to a technical challenge of using the discrete clock, and thus it requires further study. We will complete this missing component via Sambe-Howland's continuous clock, which is technically different from Ref. [23]; the key advantage of the continuous clock is that we can avoid the technicality of using localized Gaussian wave function to approximate the delta function.

This section is organized as follows. We will first review the time-independent MPF in Sec. VI A and then show how the continuous Sambe-Howland's clock can help with the conjecture from Ref. [23] in Theorem 9 in Sec. VI B. Since we had shown in precious sections that Suzuki's approach and Huyghebaert and De Raedt's approach are essentially the same in the augmented clock space, the base product formula in MPF can be straightforwardly replaced by the midpoint scheme of Huyghebaert and De Raedt, without extra effort (see Theorem 10). Though there might be other ways to establish the time-dependent MPF, the Sambe-Howland's clock offers a simple systematic approach to achieve this.

A. MPF for time-independent Hamiltonian simulation

The multiproduct formula for operator splitting was studied by Chin and Geiser [7], and contemporarily for Hamiltonian dynamics by Childs and Wiebe [8], and later further improved in Refs. [9,10]. The main idea behind this is to construct a higher-order scheme using the additive construction, namely, a linear combination of lower-order scheme with multiple time steps [72] in the way similar to the Richardson's extrapolation. For the time-independent case, one has

$$e^{-iH\Delta t} = \sum_{j=1}^{M} \alpha_j (U_2(\Delta t/k_j))^{k_j} + \mathcal{O}(\Delta t^{2m+1}), \tag{30}$$

where α_j and k_j are well chosen to satisfy conditions in Eq. (15) so as to ensure that the truncation error is $\mathcal{O}(\Delta t^{2m+1})$. The right-hand side takes the form of an LCU, which can be implemented using LCU techniques with controlled-U_2 query and additional qubits. The above $U_2(s)$ is typically chosen as the Strang-splitting scheme or say the midpoint scheme (20). Of course, U_2 can be theoretically replaced by other product formulas like any high-order symmetric product formula [48, Sec. 5], but for simplicity, we shall stick with this particular choice. There is a very recent progress to provide a detailed mathematical treatment for time-independent case [48], which showed both logarithmic error dependence and commutator scaling of MPF for *time-independent* Hamiltonian simulation.

B. MPF for time-dependent Hamiltonian simulation

The time-dependent MPF is comparatively much less studied. Suzuki's operator $\overleftarrow{\partial}/\partial t$ was adopted in Chin and Geiser [7] to formally provide a time-dependent MPF scheme, and was further explored by Geiser in Ref. [49]. They considered the operator-splitting methods for general linear dynamics without fully tailored results for quantum algorithms. Recently, Ref. [23] proposed a well-conditioned multiproduct formula by replacing the consecutive concatenation of U_2 operator via its time-dependent analog and discussed how to use LCU quantum algorithm to implement it. However, their result relies on Conjecture 1 in Ref. [23]. The technicality mentioned in their work seem to arise from adopting the discretized clock. In what follows, we will discuss how the continuous form of Sambe-Howland's clock can help with the challenge of discrete clock in Ref. [23], and also recover the scheme in Ref. [49] (which used Suzuki's time operator) with slight generalization in Theorem 10. Since the follow-up application of LCU algorithm has been well treated and explained in various literatures (e.g., [9,23,48]), we shall exclusively focus on the MPF itself, which is stated in the following theorem.

Theorem 9. Suppose α_j and k_j are chosen such that Eq. (30) holds (namely, we choose parameters for well-conditioned time-independent case). Then,

$$\mathcal{U}(t+\Delta t, t) = \sum_{j=1}^{M} \alpha_j \prod_{\ell=k_j-1}^{0} U_2\left(t + \frac{(\ell+1)\Delta t}{k_j}, t + \frac{\ell \Delta t}{k_j}\right) + \mathcal{O}(\Delta t^{2m+1}),$$

where for any $t, s \in \mathbb{T}$,

$$U_2(t,s) := \prod_{k=1}^{\Lambda} e^{-i\frac{t-s}{2}H_k(\frac{t+s}{2})} \prod_{k=\Lambda}^{1} e^{-i\frac{t-s}{2}H_k(\frac{t+s}{2})}.$$

When one has access to $\exp_{\mathcal{T}}(-i\int_{t_1}^{t_2} H_k(s)\mathrm{d}s)$ for any t_1, t_2, and k, one can use the splitting choice in Eq. (28) and end up with the following scheme:

Theorem 10. Suppose α_j and k_j are chosen such that Eq. (30) holds (namely, parameters for time-independent case). Then,

$$\mathcal{U}(t+\Delta t, t) = \sum_{j=1}^{M} \alpha_j \prod_{\ell=k_j-1}^{0} \widetilde{U}_2(t + {}^{(\ell+1)\Delta t}/_{k_j}, t + {}^{\ell\Delta t}/_{k_j}) + \mathcal{O}(\Delta t^{2m+1}),$$

where

$$\widetilde{U}_2(t,s) := \prod_{k=1}^{\Lambda} \exp_{\mathcal{T}}\left(-i\int_{s+\frac{t-s}{2}}^{t} H_k(r)\mathrm{d}r\right) \prod_{k=\Lambda}^{1} \times \exp_{\mathcal{T}}\left(-i\int_{s}^{s+\frac{t-s}{2}} H_k(r)\mathrm{d}r\right).$$

Remark 5. The base scheme can be replaced via higher-order time-independent product formulas as shown in Ref. [66] (cf. Theorem 5). As the derivations are essentially the same as the above two theorems, and our main purpose is to demonstrate the effectiveness and versatility of continuous Sambe-Howland's clock in developing quantum algorithms, we shall not pursue high-order base cases here for simplicity.

The proof of Theorem 10 is the same as Theorem 9. In the following subsection, we will show how to use both localized and delocalized formalisms to prove Theorem 9.

C. Proof of Theorem 9

The proof essentially follows the presentation of Refs. [9,48] with an application of the formalism discussed in Eq. (9) [or equivalently in Eq. (10)] in the end. Let us apply the midpoint formula (20) for the time-independent Hamiltonian $\overline{H}$ and obtain $e^{-i\overline{H}\Delta t} \approx \overline{U}_2(\Delta t)$, where

$$\overline{U}_2(\Delta t) := e^{-i\frac{\Delta t}{2}\hat{p}_s\otimes\mathbf{I}} \prod_{j=1}^{\Lambda} e^{-i\frac{\Delta t}{2}H_k(\hat{s})} \prod_{j=\Lambda}^{1} e^{-i\frac{\Delta t}{2}H_k(\hat{s})} e^{-i\frac{\Delta t}{2}\hat{p}_s\otimes\mathbf{I}}.$$

By following the derivation in Ref. [48] or simply by applying the time-independent MPF for augmented space (30), we have the following:

$$\sum_{j=1}^{M} \alpha_j \overline{U}_2(^{\Delta t}/_{k_j})^{k_j} = e^{-i\overline{H}\Delta t} + \mathcal{O}(\Delta t^{2m+1}).$$

Localized G state. By acting them on the state $|t\rangle|\phi\rangle$, one knows that

$$\sum_{j=1}^{M} \alpha_j \overline{U}_2(^{\Delta t}/_{k_j})^{k_j} |t\rangle|\phi\rangle = e^{-i\overline{H}\Delta t}|t\rangle|\phi\rangle + \mathcal{O}(\Delta t^{2m+1}).$$

By Eq. (9) (with φ being arbitrary),

$$\begin{aligned}
\langle\varphi|\mathcal{U}(t+\Delta t,t)|\phi\rangle &\overset{(9)}{=} \langle\mathbb{1}|\langle\varphi|e^{-i\overline{H}\Delta t}|t\rangle|\phi\rangle \\
&= \sum_{j=1}^{M} \alpha_j \langle\mathbb{1}|\langle\varphi|\overline{U}_2(^{\Delta t}/_{k_j})^{k_j}|t\rangle|\phi\rangle + \mathcal{O}(\Delta t^{2m+1}) \\
&= \sum_{j=1}^{M} \alpha_j \langle\varphi| \prod_{\ell=k_j-1}^{0} U_2(t+{}^{(\ell+1)\Delta t}/_{k_j}, t+{}^{\ell\Delta t}/_{k_j})|\phi\rangle + \mathcal{O}(\Delta t^{2m+1}).
\end{aligned}$$

As φ and ϕ are arbitrary, then one easily gets the final result in this theorem. We remark that to get the last line in the last equation, we used

$$\begin{aligned}
\langle\mathbb{1}|\langle\varphi|\overline{U}_2(^{\Delta t}/_{k_j})^{k_j}|t\rangle|\phi\rangle &= \langle\mathbb{1}|\langle\varphi|\overline{U}_2\left(\frac{\Delta t}{k_j}\right)^{k_j-1}|t+{}^{\Delta t}/_{k_j}\rangle|U_2(t+{}^{\Delta t}/_{k_j},t)\phi\rangle \\
&= \cdots \\
&= \langle\mathbb{1}|t+\Delta t\rangle\langle\varphi| \prod_{\ell=k_j-1}^{0} U_2(t+{}^{(\ell+1)\Delta t}/_{k_j}, t+{}^{\ell t}/_{k_j})\phi\rangle \\
&= \langle\varphi| \prod_{\ell=k_j-1}^{0} U_2(t+{}^{(\ell+1)\Delta t}/_{k_j}, t+{}^{\ell\Delta t}/_{k_j})|\phi\rangle.
\end{aligned}$$

Delocalized G state. By the delocalized version (10), one has

$$\begin{aligned}
\langle\varphi|\mathcal{U}(t+\Delta t,t)|\phi\rangle &\overset{(10)}{=} \langle t+\Delta t|\langle\varphi|e^{-i\overline{H}\Delta t}|\mathbb{1}\rangle|\phi\rangle \\
&= \sum_{j=1}^{M} \alpha_j \langle t+\Delta t|\langle\varphi|\overline{U}_2(^{\Delta t}/_{k_j})^{k_j}|\mathbb{1}\rangle|\phi\rangle + \mathcal{O}(\Delta t^{2m+1}).
\end{aligned}$$

For each term, one has

$$\begin{aligned}
\langle t+\Delta t|\langle\varphi|\overline{U}_2(^{\Delta t}/_{k_j})^{k_j}|\mathbb{1}\rangle|\phi\rangle &= \langle t+\Delta t|\langle\varphi|\overline{U}_2(^{\Delta t}/_{k_j})\overline{U}_2(^{\Delta t}/_{k_j})^{k_j-1}|\mathbb{1}\rangle|\phi\rangle \\
&= \langle t+\Delta t-{}^{\Delta t}/_{k_j}|(\langle\varphi|U_2(t+\Delta t, t+\Delta t-{}^{\Delta t}/_{k_j}))\overline{U}_2(^{\Delta t}/_{k_j})^{k_j-1}|\mathbb{1}\rangle|\phi\rangle \\
&= \cdots \\
&= \langle t|\left(\langle\varphi| \prod_{\ell=k_j-1}^{0} U_2(t+{}^{(\ell+1)\Delta t}/_{k_j}, t+{}^{\ell\Delta t}/_{k_j})\right)|\mathbb{1}\rangle|\phi\rangle \\
&= \langle\varphi| \prod_{\ell=k_j-1}^{0} U_2(t+{}^{(\ell+1)\Delta t}/_{k_j}, t+{}^{\ell\Delta t}/_{k_j})|\phi\rangle.
\end{aligned}$$

By combining the last two questions, one arrives at the same conclusion as the localized version (9).

VII. TIME-DEPENDENT qDRIFT

In this section, we will demonstrate that by applying qDrift [14], initially developed by Campbell for time-independent Hamiltonian simulation, to the augmented Sambe-Howland's clock space, we can readily develop time-dependent qDrift algorithms. We would like to emphasize that similar calculations can also been carried on to randomized permutation [13] and partially randomized algorithm [51,52] without theoretical challenge (which we shall not further pursue here for clarity).

This section is organized as follows. We will first review the idea of qDrift in Sec. VII A for time-independent Hamiltonian simulation. With Sambe-Howland's clock, we can immediately generalize qDrift to the time-dependent case in Secs. VII B and VII C. We remark that even though such a generalization can also been conjectured and validated without Sambe-Howland's clock, this generic framework, nevertheless, provides a unifying and systemic approach for such algorithms built on random quantum circuit. More importantly, estimating the error is no different from the time-independent case. Finally, in Sec. VII D, we will establish the connection between time-dependent qDrift developed using Sambe-Howland's clock and the continuous qDrift in Ref. [26]. For the setup of digitized adiabatic simulation, we will show that "continuous qDrift" proposed in Ref. [26] is almost equivalent to applying the time-independent qDrift in the augmented Sambe-Howland's clock Hamiltonian (see Lemma 14).

A. Review of qDrift for the time-independent case

We first recall the qDrift for the time-independent Hamiltonian with the form given in Eqs. (2) and (3), where $f_k(s)$ is time-independent [namely, $f_k(s) \equiv f_k$ is simply a constant]. Reference [14] proposed the qDrift algorithm, which rewrites the unitary evolution (in the density matrix formalism) as the expectation of local unitary evolution, which can then be realized via random unitary circuits. More specifically, we consider the following decomposition:

$$H = \sum_k \lambda_k \left(\frac{H_k}{\lambda_k} \right),$$

and the qDrift algorithm uses the following approximation:

$$e^{-i\Delta t H} \rho\, e^{i\Delta t H} = \sum_k \lambda_k e^{-i\Delta t \frac{H_k}{\lambda_k}} \rho e^{i\Delta t \frac{H_k}{\lambda_k}} + \mathcal{O}(\Delta t^2), \tag{31}$$

where λ_j is an arbitrary nondegenerate discrete probability distribution. The key advantage of this qDrift algorithm comes from a well-chosen probability distribution to balance the magnitude of f_j. For instance, when $\|\boldsymbol{h}_k\| = \mathcal{O}(1)$, one can choose $\lambda_j := |f_j| / \sum_k |f_k|$ so that the final approximation error scales with respect to $\sum_k |f_k|$, rather than directly depending on the number of local Hamiltonian terms Λ.

This idea can be straightforwardly generalized to infinite many terms. Suppose that there is a probability space with event ω such that the Hamiltonian can be written as the expectation of a collection of "local Hamiltonians" H_ω as follows:

$$H = \mathbb{E}_\omega[H_\omega] \equiv \int \mathrm{d}\omega\, \lambda(\omega) H_\omega,$$

where H_ω is a Hermitian operator and $\lambda(\omega)$ is a nondegenerate probability distribution on a certain set of indices. Then, the above estimate (31) can be essentially rewritten as

$$\underbrace{e^{-i\Delta t H} \rho\, e^{i\Delta t H}}_{=:\, \mathcal{U}_{\Delta t}(\rho)} = \underbrace{\int \mathrm{d}\omega\, \lambda(\omega) e^{-i\Delta t H_\omega}\, \rho\, e^{i\Delta t H_\omega}}_{=:\, \mathcal{E}_{\lambda,\Delta t}(\rho)} + \mathcal{O}(\Delta t^2). \tag{32}$$

The detailed error analysis has been investigated in Ref. [14] and more comprehensive analysis in Ref. [73], which can be applied to analyze the error in the last equation.

We collect some facts:

Lemma 11. Denote the measure $\eta(\omega_1, \omega_2) = \lambda(\omega_1)(\lambda(\omega_2) - \delta(\omega_1 - \omega_2))$. The distance between the above two channels is bounded above by

$$\|\mathcal{U}_{\Delta t} - \mathcal{E}_{\lambda,\Delta t}\|_1 \leqslant \frac{\Delta t^2}{2} C + \mathcal{O}(\Delta t^3),$$

where

$$C = \iint \mathrm{d}\omega_1 \mathrm{d}\omega_2\, |\eta|(\omega_1, \omega_2)\, \|[H_{\omega_1}, [H_{\omega_2}, \cdot]]\|_1.$$

The proof only involves direct computation and is postponed to Appendix A 5. Given estimates about right nested commutator of $[H_{\omega_1}, [H_{\omega_2}, \cdot]]$, one could choose the probability measure λ such that the right-hand side is minimized.

B. Time-dependent qDrift using Sambe-Howland's clock (I)

For the general time-dependent Hamiltonian H as in Eq. (2) and a general discrete probability distribution $\{\lambda_k\}_{k=1}^{\Lambda}$, let us consider the following decomposition:

$$\overline{H} = \sum_{k=1}^{\Lambda} \lambda_k \underbrace{\left(\hat{p}_s \otimes \mathbf{I} + \frac{1}{\lambda_k} H_k(\hat{s}) \right)}_{=:\widetilde{H}_k}. \tag{33}$$

By applying the above time-independent qDrift algorithm (32) for the augmented Hamiltonian $\overline{H}$, one has

$$\begin{aligned} \mathcal{U}(t+\Delta t, t)\, \rho\, \mathcal{U}(t+\Delta t, t)^\dagger &\overset{(10)}{=} \langle t+\Delta t|_s e^{-i\overline{H}\Delta t}\, (|\mathbb{1}\rangle\langle\mathbb{1}| \otimes \rho)\, e^{i\overline{H}\Delta t} |t+\Delta t\rangle_s \\ &\overset{(32)}{=} \sum_k \lambda_k\, \langle t+\Delta t|_s e^{-i\Delta t \widetilde{H}_k} (|\mathbb{1}\rangle\langle\mathbb{1}| \otimes \rho)\, e^{i\Delta t \widetilde{H}_k} |t+\Delta t\rangle_s + \mathcal{O}(\Delta t^2) \end{aligned}$$

$$= \sum_k \lambda_k \, \langle t+\Delta t|_s e^{-i\Delta t(\hat{p}_s\otimes \mathbf{I}+\frac{1}{\lambda_k}H_k(\hat{s}))}(|\mathbb{1}\rangle\langle\mathbb{1}|\otimes\rho)\, e^{i\Delta t(\hat{p}_s\otimes \mathbf{I}+\frac{1}{\lambda_k}H_k(\hat{s}))}|t+\Delta t\rangle_s + \mathcal{O}(\Delta t^2)$$

$$\overset{(10)}{=} \sum_k \lambda_k \, e_{\mathcal{T}}^{-i\int_t^{t+\Delta t}\lambda_k^{-1}H_k(s)\mathrm{d}s} \, \rho \, e_{\mathcal{T}}^{i\int_t^{t+\Delta t}\lambda_k^{-1}H_k(s)\mathrm{d}s} + \mathcal{O}(\Delta t^2).$$

This suggests the approximation

$$\mathcal{U}(t+\Delta t,t)\,\rho\,\mathcal{U}(t+\Delta t,t)^\dagger \approx \mathcal{E}_{\lambda,t,\Delta t}(\rho), \tag{34}$$

where the latter quantum channel is defined as

$$\mathcal{E}_{\lambda,t,\Delta t}(\rho) := \sum_k \lambda_k \, e_{\mathcal{T}}^{-i\int_t^{t+\Delta t}\lambda_k^{-1}H_k(s)\mathrm{d}s} \, \rho \, e_{\mathcal{T}}^{i\int_t^{t+\Delta t}\lambda_k^{-1}H_k(s)\mathrm{d}s}. \tag{35}$$

This immediately generalizes the time-independent qDrift (31) to the time-dependent Hamiltonian simulation. One can immediately check that the error scales like the following:

Lemma 12. Suppose the time-dependent Hamiltonian has the form in Eqs. (2) and (3). The error between approximated state and the exact state is

$$\|\mathcal{U}(t+\Delta t,t)\rho\mathcal{U}(t+\Delta t,t)^\dagger - \mathcal{E}_{\lambda,t,\Delta t}(\rho)\|_1 \leqslant \frac{C\Delta t^2}{2} + \mathcal{O}(\Delta t^3),$$

where

$$C = \sum_{k_1,k_2} \left|\lambda_{k_2} - \delta_{k_1,k_2}\right| \frac{\left|f_{k_1}(t+\Delta t)f_{k_2}(t+\Delta t)\right|}{\lambda_{k_2}} \left\|\left[\boldsymbol{h}_{k_1},\left[\boldsymbol{h}_{k_2},\rho\right]\right]\right\|_1.$$

The detailed proof is postponed to Appendix A 5. With estimates of the upper bound of C, one can adaptively choose the time step Δt, as well as find the optimal probability distribution on the fly.

C. Time-dependent qDrift using Sambe-Howland's clock (II)

Suppose that we consider the following probability space with events $\omega = (k, r) \in \{1, 2, \ldots, \Lambda\} \times [0, 1]$ following a nondegenerate discrete and continuous hybrid distribution μ. Let us consider a more complex decomposition,

$$\begin{aligned}\overline{H} &= \sum_{k=1}^{\Lambda}\int_0^1 \mathrm{d}r\, \mu(k,r)\left(\hat{p}_s\otimes\mathbf{I} + \frac{H_k(\hat{s})}{\mu(k,r)}\right)\\ &= \mathbb{E}_\omega \underbrace{(\hat{p}_s\otimes\mathbf{I} + H_\omega(\hat{s}))}_{=:\widetilde{H}_\omega},\end{aligned} \tag{36}$$

where $H_\omega(\hat{s}) = \frac{H_k(\hat{s})}{\mu(k,r)}$ for this example. When $\mu(k, r) \equiv \lambda_k$ is independent of r, then this decomposition simply reduces to the above (33). By applying the qDrift algorithm (32) to the Hamiltonian decomposition (36) in the augmented space, we have the following approximations:

$$\begin{aligned}\mathcal{U}(t+\Delta t,t)\rho\,\mathcal{U}(t+\Delta t,t)^\dagger &\overset{(10)}{=} \langle t+\Delta t|_s e^{-i\overline{H}\Delta t}(|\mathbb{1}\rangle\langle\mathbb{1}|\otimes\rho)e^{i\overline{H}\Delta t}|t+\Delta t\rangle_s\\ &\overset{(32)}{=} \mathbb{E}_\omega\langle t+\Delta t|_s e^{-i\Delta t\widetilde{H}_\omega}(|\mathbb{1}\rangle\langle\mathbb{1}|\otimes\rho)e^{i\Delta t\widetilde{H}_\omega}|t+\Delta t\rangle_s + \mathcal{O}(\Delta t^2)\\ &= \mathbb{E}_\omega\langle t+\Delta t|_s e^{-i\Delta t(\hat{p}_s\otimes\mathbf{I}+H_\omega(\hat{s}))}(|\mathbb{1}\rangle\langle\mathbb{1}|\otimes\rho)e^{i\Delta t(\hat{p}_s\otimes\mathbf{I}+H_\omega(\hat{s}))}|t+\Delta t\rangle_s + \mathcal{O}(\Delta t^2)\\ &= \sum_k\int_0^1 \mathrm{d}r\,\mu(k,r) e_{\mathcal{T}}^{-i\frac{\int_t^{t+\Delta t}H_k(s)\mathrm{d}s}{\mu(k,r)}}\rho e_{\mathcal{T}}^{i\frac{\int_t^{t+\Delta t}H_k(s)\mathrm{d}s}{\mu(k,r)}} + \mathcal{O}(\Delta t^2).\end{aligned}$$

This suggests the approximation

$$\mathcal{U}(t+\Delta t,t)\,\rho\,\mathcal{U}(t+\Delta t,t)^\dagger \approx \mathcal{E}_{\mu,t,\Delta t}(\rho),$$

where

$$\mathcal{E}_{\mu,t,\Delta t}(\rho) = \sum_k\int_0^1 \mathrm{d}r\,\mu(k,r)\, e_{\mathcal{T}}^{-i\frac{\int_t^{t+\Delta t}H_k(s)\mathrm{d}s}{\mu(k,r)}}\,\rho\, e_{\mathcal{T}}^{i\frac{\int_t^{t+\Delta t}H_k(s)\mathrm{d}s}{\mu(k,r)}}. \tag{37}$$

Lemma 13. Suppose the time-dependent Hamiltonian has the form in Eqs. (2) and (3). The error between approximated state and the exact state is

$$\|\mathcal{U}(t+\Delta t,t)\rho\mathcal{U}(t+\Delta t,t)^\dagger - \mathcal{E}_{\mu,t,\Delta t}(\rho)\|_1 \leqslant \frac{C\Delta t^2}{2} + \mathcal{O}(\Delta t^3),$$

where

$$C = \iint \mathrm{d}\omega_1 \mathrm{d}\omega_2 \left(|\mu(\omega_2) - \delta(\omega_1 - \omega_2)| \frac{\left| f_{k_1}(t+\Delta t) f_{k_2}(t+\Delta t) \right|}{\mu(\omega_2)} \left\| \left[\boldsymbol{h}_{k_1}, \left[\boldsymbol{h}_{k_2}, \cdot \right] \right] \right\|_1 \right),$$

and $\omega_1 = (k_1, r_1)$, $\omega_2 = (k_2, r_2)$, and $\iint \mathrm{d}\omega = \sum_k \int_0^1 \mathrm{d}r$.

See Appendix A 5 for detailed proof.

D. Connections to continuous qDrift

The above noisy channels (35) and (37) can be regarded as reasonable ways to generalize the original time-independent qDrift to time-dependent case. Another possibility, known as the "continuous qDrift," was proposed in Ref. [26, Eq. (77)]:

$$\mathcal{E}^{(\text{c-qDrift})}_{q,t,\Delta t}(\rho) := \sum_k \int_0^1 \mathrm{d}\tau q(k,\tau)\, e^{-i\Delta t \frac{H_k(t+\tau\Delta t)}{q(k,\tau)}} \rho e^{i\Delta t \frac{H_k(t+\tau\Delta t)}{q(k,\tau)}}, \tag{38}$$

where q is a probability measure on the same discrete-continuous hybrid probability space. As a remark, for consistency of notations, we have slightly changed notations in Ref. [26, Eq. (77)] and rescaled the "probability distribution $p_\ell(\tau)$" in their equation from $[0, \Delta t]$ to the range $\tau \in [0, 1]$ above.

In general, by comparing the formalism in Eqs. (37) and (38), we can observe that the continuous qDrift can be obtained by performing the following approximation for any $\tau \in [0, 1]$:

$$e^{-i\frac{\int_t^{t+\Delta t} H_k(s)\mathrm{d}s}{\mu(k,r)}}_{\mathcal{T}} = e^{-i\Delta t \frac{H_k(t+\tau\Delta t)}{\mu(k,\tau)}} + \mathcal{O}(\Delta t^2).$$

This is essentially Lie's first-order approximation using the time grid point $t + \tau\Delta t$.

We are particularly interested in time-dependent Hamiltonian simulation for digitized adiabatic simulation with the form in Eqs. (2) and (3). In this setup, despite that Eq. (37) uses the integration-based query and Eq. (38) uses the pointwise query, the formalism in Eqs. (37) and (38) are equivalent after rescaling.

Lemma 14. Suppose the time-dependent Hamiltonian has the form in Eqs. (2) and (3). We further assume that $f_k(s) > 0$ for any k and time $s \in [t, t + \Delta t]$. Then, for any arbitrary probability measure μ, there exists a measure q such that

$$\mathcal{E}_{\mu,t,\Delta t} = \mathcal{E}^{(\text{c-qDrift})}_{q,t,\Delta t}.$$

Namely, applying qDrift for Sambe-Howland's clock using decomposition (36) leads into continuous qDrift in Ref. [26].

See Appendix A 5 for detailed proof.

VIII. TAYLOR'S EXPANSION-BASED ALGORITHMS

This section aims to illustrate the compatibility of Sambe-Howland's clock for LCU-Taylor based algorithms. We shall first discuss existing Dyson's expansion-based methods, which might be hard to implement in the near future due to the black-box type of oracle query. As the Hamiltonian $\overline{H}$ is essentially time-independent, we consider a direct application of Taylor's expansion to Sambe-Howland's clock and present the resulting quantum algorithms based on LCU models. The latter one is not the same as applying Dyson's expansion. We aim to illustrate that LCU-Taylor based quantum algorithms are compatible with Sambe-Howland's clock, which further confirms the versatility of this general approach in developing quantum algorithms for time-dependent dynamics.

A. Related works

Assuming that the Hamiltonian has the form of linear combination of unitaries [e.g., assume that $\boldsymbol{h}_j$ in Eq. (3) are unitary] and H is time-independent, Ref. [15] provided a simple method based on Taylor's expansion to achieve Hamiltonian simulation with $\mathcal{O}(\frac{T\log(T/\epsilon)}{\log\log(T/\epsilon)})$ queries to controlled-$\boldsymbol{h}_j$ gates and other two-qubit gates, where T is the length of simulation time.

The time-dependent generalization has been studied in Refs. [29,56] using Dyson's series, which is the generalization of Taylor's expansion by considering the time ordering of Hamiltonians. If one discretizes the Hamiltonian $H(s)$ at grid points $t_j = j\frac{t}{M}$ $(1 \leqslant j \leqslant M)$ and for time-dependent Hamiltonian simulation, one has to use all information from $H(s)$ to simulate the dynamics, which motivated Ref. [29] to use oracle queries to HAM, defined as follows:

$$\langle 0|_a \mathrm{HAM} |0\rangle_a = \frac{1}{\alpha} \sum_{m=0}^{M-1} |m\rangle\langle m| \otimes H\left(\frac{mt}{M}\right), \tag{39}$$

where $\alpha := \sup_{s\in[0,T]} \|H(s)\|$; see Definition 2 in Ref. [29]. For a given error tolerance ϵ, it has been shown in, e.g., Refs. [29,56] that one requires $M = \Theta(1/\epsilon)$ [29, Lemma 5]. Reference [29, Theorem 3] showed that the required number of queries to HAM logarithmically depends on the error ϵ. However, the less discussed issue is that during implementation, the gate cost for HAM may scale as $\mathcal{O}(1/\epsilon)$ in the worst case. In Ref. [56], they showed similar results and the actual implementation of oracle queries appear to be not explicitly explained. Such a framework has been further generalized to develop first-order [58] and second-order [59] algorithms based on the Magnus expansion.

B. The second-order Taylor-based algorithm for Sambe-Howland's clock

In this part, we will discuss quantum algorithms based on Sambe-Howland's clock using second-order Taylor's expansion, which complements the aforementioned Dyson's expansion [29,56] and the recent works using Magnus's expansion [58,59]. Its generalization to high-order cases should merely be a routine task, if one only aims at finding a finite-order algorithm. As mentioned above, we present such an algorithm for illustration only to provide a more complete picture of how Sambe-Howland's clock can help with developing quantum algorithms. As a remark, we shall assume that $\boldsymbol{h}_j$ is unitary throughout this subsection.

By applying Taylor's expansion directly to Sambe-Howland's clock, we have the following:

$$e^{-i\Delta t\overline{H}} = \mathbf{I} - i\Delta t\left(\hat{p}_s \otimes \mathbf{I} + \sum_{j=1}^{\Lambda} f_j(\hat{s})\boldsymbol{h}_j\right) + \frac{-\Delta t^2}{2}\left(\hat{p}_s \otimes \mathbf{I} + \sum_{j=1}^{\Lambda} f_j(\hat{s})\boldsymbol{h}_j\right)^2 + \mathcal{O}(\Delta t^3).$$

By applying the delocalized version (10),

$$\begin{aligned}
&\mathcal{U}(t+\Delta t, t)\\
&= \langle t+\Delta t|e^{-i\overline{H}\Delta t}|\mathbb{1}\rangle\\
&= \mathbf{I} - i\Delta t\left(\sum_{j=1}^{\Lambda} f_j(t+\Delta t)\boldsymbol{h}_j\right)\\
&\quad + \frac{-\Delta t^2}{2}\left(-i\sum_{j=1}^{\Lambda} f_j'(t+\Delta t)\boldsymbol{h}_j\right.\\
&\quad \left. + \sum_{j,k} f_j(t+\Delta t)f_k(t+\Delta t)\boldsymbol{h}_j\boldsymbol{h}_k\right) + \mathcal{O}(\Delta t^3)\\
&= \mathbf{I} + \sum_{j=1}^{\Lambda}\left(\Delta t f_j(t+\Delta t) - \frac{\Delta t^2}{2}f_j'(t+\Delta t)\right)(-i\boldsymbol{h}_j)\\
&\quad + \sum_{j,k=1}^{\Lambda}\frac{\Delta t^2 f_j(t+\Delta t)f_k(t+\Delta t)}{2}(-i\boldsymbol{h}_j)(-i\boldsymbol{h}_k) + \mathcal{O}(\Delta t^3)\\
&=: \mathcal{U}_{\text{Taylor}}(t+\Delta t, t) + \mathcal{O}(\Delta t^3).
\end{aligned} \tag{40}$$

Since $\boldsymbol{h}_j$ are Hermitian and unitary, it is clear that $-i\boldsymbol{h}_j$ are also unitary, and the above equation approximates the unitary evolution $\mathcal{U}(t+\Delta t, t)$ in the form of LCU. This expansion can also been obtained by Dyson's expansion, with further approximation of the integration at the time $t+\Delta t$.

For simplicity, let us consider the case where $f_j \geqslant 0$ and Δt is small enough such that $\Delta t f_j(t+\Delta t) - \frac{\Delta t^2}{2}f_j'(t+\Delta t) \geqslant 0$. Then, the success probability for constructing the gate using LCU directly [15] is $1/\mathsf{s}^2$ where s is simply the summation of coefficients:

$$\begin{aligned}
\mathsf{s} &= 1 + \sum_{j=1}^{\Lambda}\left(\Delta t f_j(t+\Delta t) - \frac{\Delta t^2}{2}f_j'(t+\Delta t)\right)\\
&\quad + \sum_{j,k=1}^{\Lambda}\frac{\Delta t^2 f_j(t+\Delta t)f_k(t+\Delta t)}{2}\\
&= e^{\sum_{j=1}^{\Lambda}\int_t^{t+\Delta t} f_j(s)\,\mathrm{d}s} + \mathcal{O}(\Delta t^3).
\end{aligned}$$

The challenge of vanishing probability. Suppose we consider the time interval $[\mathsf{T}_i, \mathsf{T}_f]$, by discretizing the time into N subintervals $\mathsf{T}_i = t_0 < t_1 < \cdots t_N = \mathsf{T}_f$, and along multiple iterations, one may prepare the state proportional to

$$\begin{aligned}
&\mathcal{U}_{\text{Taylor}}(t_N, t_{N-1})\mathcal{U}_{\text{Taylor}}(t_{N-1}, t_{N-2})\cdots\mathcal{U}_{\text{Taylor}}(t_1, t_0)|\psi\rangle\\
&\quad \approx \mathcal{U}(\mathsf{T}_f, \mathsf{T}_i)|\psi\rangle + \mathcal{O}(\Delta t^2),
\end{aligned}$$

with success probability asymptotically

$$\exp\left(-2\sum_{j=1}^{\Lambda}\int_{\mathsf{T}_i}^{\mathsf{T}_f} f_j(s)\,\mathrm{d}s\right).$$

This probability vanishes exponentially fast with respect to $\mathsf{T}_f - \mathsf{T}_i$, which is also well discussed in various literatures, e.g., [74].

Application of oblivious amplitude amplification. Suppose that we consider the simulation on the time interval $[0, T]$ where T is large (or equivalently the magnitude of f_j is large while $T = \mathcal{O}(1)$), we can always find some special time grid pints $\mathsf{T}_1 \equiv 0, \mathsf{T}_1, \ldots, \mathsf{T}_\beta$ such that

$$e^{-2\sum_{j=1}^{\Lambda}\int_{\mathsf{T}_k}^{\mathsf{T}_{k+1}} f_j(s)\,\mathrm{d}s} = 1/4.$$

For simplicity, let us suppose that $\mathsf{T}_\beta = T$. Then, with at most three walk operators (constructed via controlled-$\boldsymbol{h}_j^{(\dagger)}$ gates) and some reflection operators, one can boost the probability of the above LCU-Taylor scheme to one for the time interval $[\mathsf{T}_k, \mathsf{T}_{k+1}]$ where $0 \leqslant k < \beta - 1$. With the relation

$$\sum_{j=1}^{\Lambda}\int_0^T f_j(s)\,\mathrm{d}s = \beta\ln(2),$$

the number of times needed to apply oblivious amplitude amplification is $\mathcal{O}(T)$.

To obtain a heuristic estimate of the resources, within each subinterval $[\mathsf{T}_k, \mathsf{T}_{k+1}]$, the error from the LCU-Taylor should be confined to $\mathcal{O}(\epsilon/T)$ and therefore, the time-interval $\Delta t = \mathcal{O}(\sqrt{\epsilon/T})$. For each construction of LCU in Eq. (40), the application of controlled-$\boldsymbol{h}_j$ gates (as well as controlled-$\boldsymbol{h}_j^\dagger$) scales at most like $\mathcal{O}(\Lambda^2)$ and therefore, the total gate complexity scales like $\mathcal{O}(\Lambda^2\frac{T}{\Delta t}) = \mathcal{O}(\Lambda^2 T\sqrt{T/\epsilon})$. If one keeps Taylor's expansion up to the order p (without further optimization), then the scaling is expected to be at most $\mathcal{O}(T^{1+\frac{1}{p}}\Lambda^p\epsilon^{-1/p})$ in a way similar to product formulas.

The above arguments suggest that one can avoid the vanishing probability problem and there is no need to encode the whole time-dependent Hamiltonian into a single large unitary matrix as in Eq. (39). The above discussion illustrates how time-dependent Hamiltonian simulation based on the LCU-Taylor could be achieved using Sambe-Howland's clock and with a designing principle similar to time-independent LCU-Taylor [15].

IX. NUMERICAL EXPERIMENTS

In this section, we will validate the practical efficacy of product-based formula derived based on Sambe-Howland's clock in handling the time dependence. We consider two digitized adiabatic simulation problems (adiabatic Grover's algorithm and adiabatic Google's PageRank algorithm). An additional experiment will be presented in Appendix B 2 for time-dependent quantum Ising chain. Numerical experiments suggest that the generalized high-order HDR algorithms can overall achieve the best performance or near best

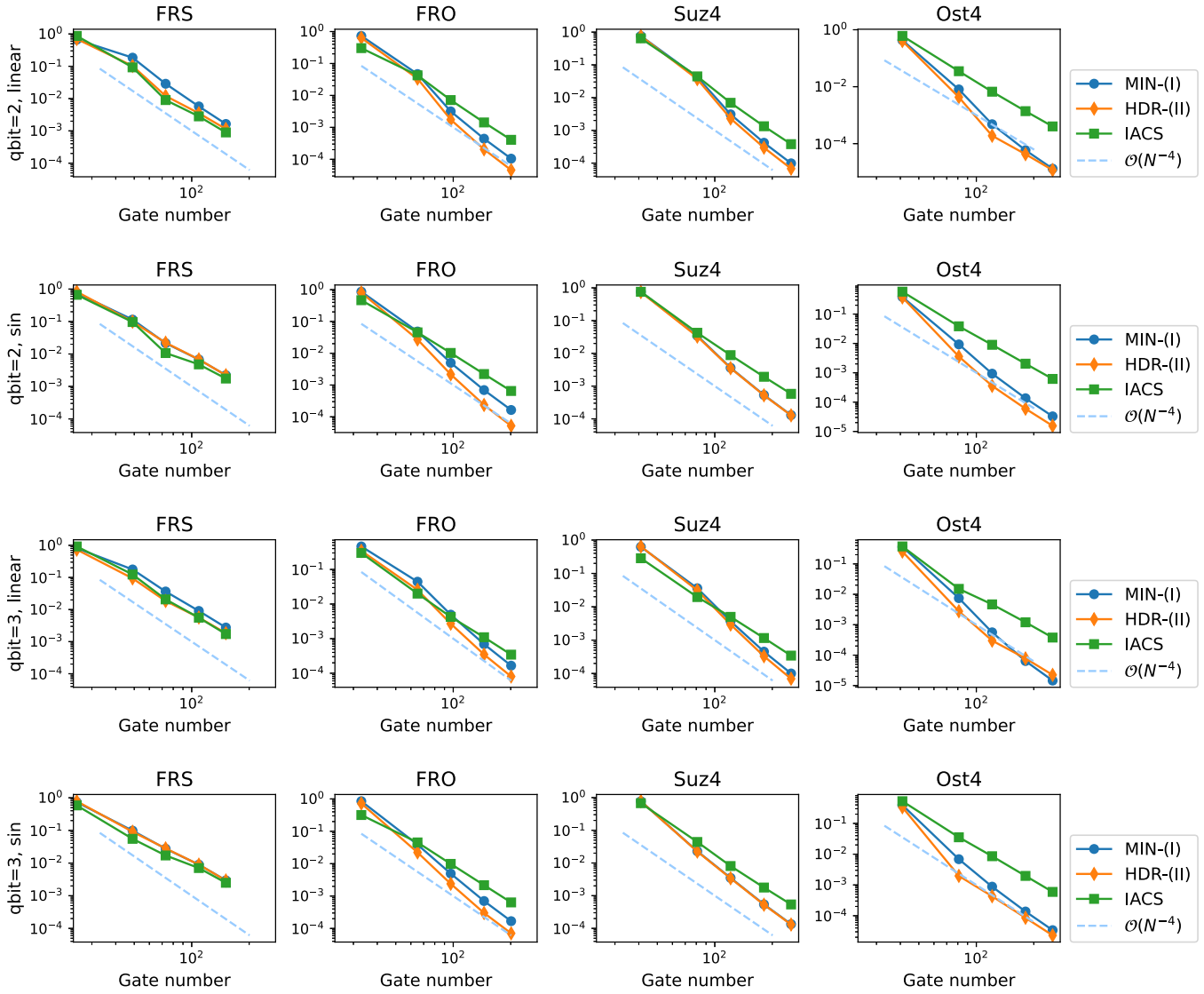


FIG. 1. Averaged simulation error (in trace distance) for Grover's search algorithm with respect to the gate counts N for various time-dependent schemes. "MIN-(I)" refers to the scheme in Eq. (23) with the ordering H_1, $\hat{p}$, and H_2. HDR refers to the scheme in Eq. (29). IACS refers to the scheme in Ref. [27]; see Eq. (26). The blue dashed line indicates the scaling $\mathcal{O}(N^{-4})$ and is the same for all subplots.

performance; for some parameter regions, it can achieve significantly improved performance than a Magnus-based algorithm recently proposed in Ref. [27]. We use four different weights "FRS," "FRO," "Suz4," and "Ost4" from time-independent product formulas (all being fourth-order schemes) [66]; see Ref. [66] or Appendix B 1 for details. For these examples, we consider $H(t) = f_1(t)\boldsymbol{h}_1 + f_2(t)\boldsymbol{h}_2$ for $t \in [0, 1]$, and assume access to $e^{-i\alpha \boldsymbol{h}_k}$ for any $\alpha \in \mathbb{R}$ and $k = 1, 2$. The gate count refers to the number of such unitaries that we need. We remark that this is still a fair comparison since all algorithms considered below need to use such resources; a further decomposition into one-qubit and two-qubit gates are not considered herein for simplicity, as we only aim at comparing the relative performance of algorithms in handling the time dependence. As mentioned earlier in the introduction, broader benchmark tests are undoubtedly necessary for more thorough validation. However, the existing experiments have already demonstrated the potential of Sambe-Howland's clock in aiding the development of efficient quantum algorithms.

A. Adiabatic Grover's algorithm

Suppose that we want to prepare the n-qubit state $|\varphi\rangle = |\varphi_1\rangle|\varphi_2\rangle \cdots |\varphi_n\rangle$ via the following Hamiltonians:

$$\boldsymbol{h}_1 = \mathbf{I} - |+\rangle^{\otimes n}\langle +|^{\otimes n}, \quad \boldsymbol{h}_2 = \mathbf{I} - |\varphi\rangle\langle\varphi|,$$

where we choose $|\varphi\rangle$ as a product of n local pure states in numerical experiments and $|+\rangle$ is the maximally entangled state $|+\rangle = \frac{1}{\sqrt{2}}(|0\rangle + |1\rangle)$. We consider the following adiabatic path:

$$H(t) = T((1 - f(t))\boldsymbol{h}_1 + f(t)\boldsymbol{h}_2), \quad t \in [0, 1],$$

where we choose $T = 40$ in experiments, and the schedule is simply chosen as

$$f(t) = \begin{cases} t, & \text{(linear)}, \\ \sin\left(\frac{\pi}{2}t\right), & \text{(sin)}. \end{cases} \tag{41}$$

The averaged simulation error in trace distance for Grover's search algorithm (without considering the adiabatic

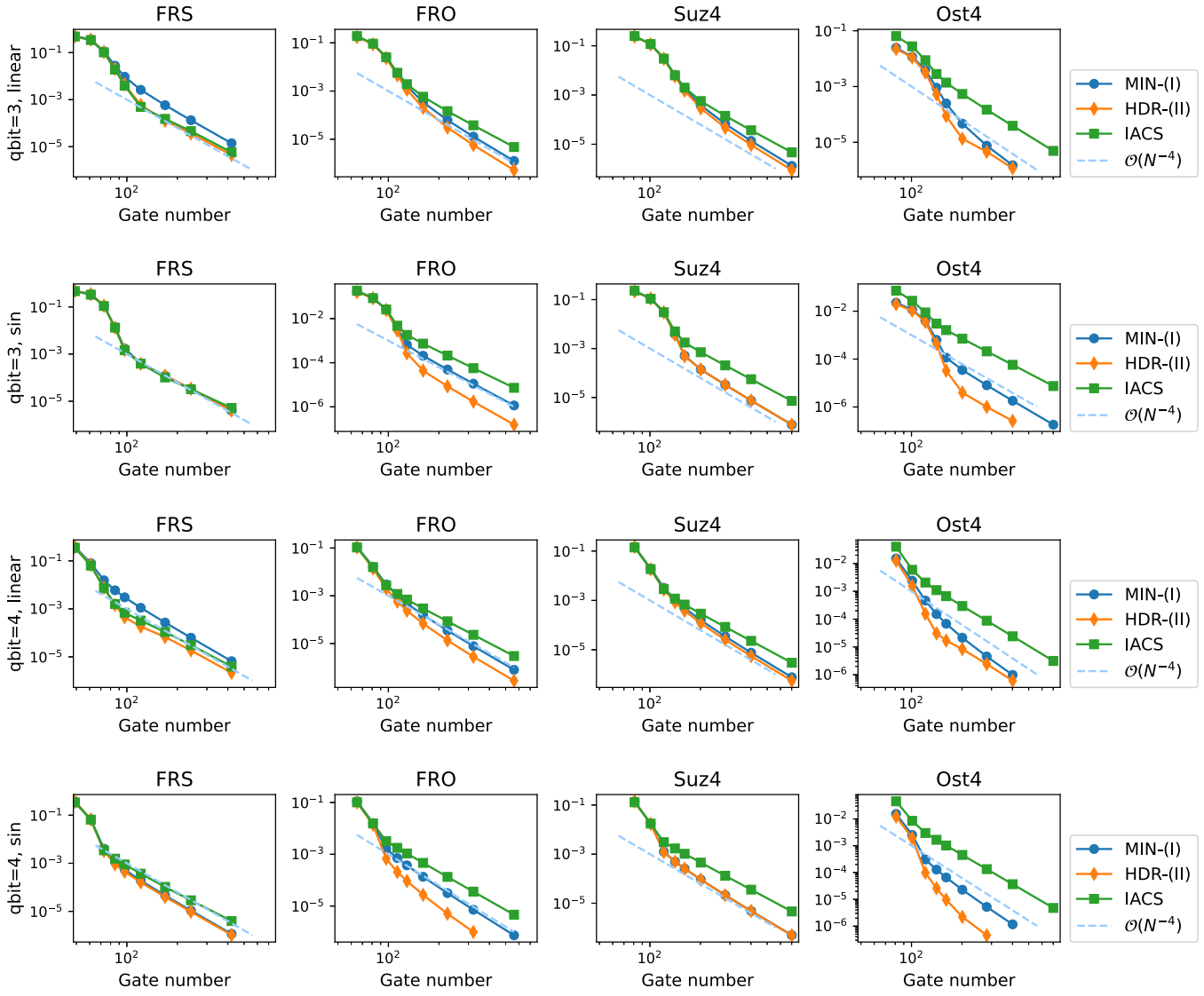


FIG. 2. Averaged simulation error in trace distance for adiabatic Google's PageRank algorithm with respect to the gate counts N for various time-dependent schemes. "MIN-(I)" refers to the scheme (23) with the ordering H_1, $\hat{p}$, and H_2. HDR refers to the scheme in Eq. (29). IACS refers to the scheme in Ref. [27]; see also Eq. (26). The blue dashed line indicates the scaling $\mathcal{O}(N^{-4})$ and is the same for all subplots.

approximation error) is visualized in Fig. 1. The error has been averaged over 17, 16, 13, and 5 randomly generated target states $|\varphi\rangle$ such that $|\langle\varphi(1)|\varphi\rangle|^2 \geqslant 99\%$, where $\varphi(1)$ is the exact state generated by the digital adiabatic simulation. As can be seen in Fig. 1, IACS (a Magnus-motivated product formula) may perform better if one uses a less efficient weight scheme like FRS. However, it does not improve much using a more efficient weight scheme. This can be possibly explained as follows: since the total error of Magnus-based product formula comes from both the Magnus expansion and the additional application of the product formula, a more efficient weight scheme can provide little help with reducing the error of Magnus's expansion itself. However, this is likely not an issue for a pure product-based formula (using Sambe-Howland's clock); with optimized time-independent product formula, one can generally expect a more efficient time-dependent product formula (as demonstrated in this example). We can observe that the HDR algorithm generally provides the best performance in most parameter regions, and it can offer roughly an order of magnitude improvement compared with IACS scheme using "Ost4" weights.

B. Adiabatic Google's PageRank algorithm

The second example is the adiabatic Google's PageRank algorithm. Suppose we have a directed graph of nodes (e.g., web pages) with adjacency matrix A (whose dimension is 2^n for simplicity), the transition probability for the random walk on the graph is defined as

$$P(i,j) = \begin{cases} 1/d(i), & \text{if } d(i) > 0 \quad \text{and} \quad (i,j) \text{ is an edge;} \\ 0, & \text{if } d(i) > 0 \quad \text{and} \quad (i,j) \text{ is not an edge;} \\ 1/2^n, & \text{if } d(i) = 0; \end{cases}$$

where $d(i)$ is the out degree for the node $i = 0, 1, \ldots, 2^n - 1$. The Google matrix G is defined as $G = \alpha P^T + (1-\alpha)E$, where $\alpha = 0.85$ typically and E is a matrix filled with elements $1/2^n$ [28,75]. The stationary distribution of G, denoted

as $|\varphi\rangle$, satisfies $G|\varphi\rangle = |\varphi\rangle$, and it characterizes the importance of these nodes. Similar to previous examples, it can be solved adiabatically, e.g., using the following two Hamiltonians:

$$\boldsymbol{h}_1 = \mathbf{I} - |+\rangle^{\otimes n}\langle +|^{\otimes n}, \quad \boldsymbol{h}_2 = (\mathbf{I} - G)^\dagger(\mathbf{I} - G).$$

We consider the same schedule as in Grover's case with time schedule chosen as in Eq. (41) and timescale $T = 40$ for experiments, and $n = 3, 4$ (namely, 8 nodes and 16 nodes, respectively). The simulation error for various cases (without adiabatic approximation error) is summarized in Fig. 2. The error has been averaged over 15 randomly generated graphs; we have validated the high fidelity for all such cases $|\langle\varphi(1)|\varphi\rangle|^2 \geqslant 99\%$, where $|\varphi\rangle$ is the ground state of $\boldsymbol{h}_2$ (namely, the page-rank vector) and $\varphi(1)$ is the approximated state from the adiabatic simulation. In Fig. 2, one can observe that the generalized HDR algorithm consistently has comparable performance compared with IACS scheme, and it outperforms significantly when equipped with a very efficient time-independent scheme "Ost4." Across a variety of precision-level and different weights (from time-independent schemes), the fourth-order HDR algorithm (29) seems to be the most reliable and efficient one in general.

X. SUMMARY

In this work, we have used "Sambe-Howland's continuous clock" to develop quantum algorithms for analog quantum computing and digital quantum computing, which complements recent advances using Sambe's space in Refs. [24,25,67]. In particular, for digital quantum computing, we have demonstrated that Sambe-Howland's clock offers a way to unify the approach by Suzuki and the approach by Huyghebaert and De Raedt. Moreover, this extra continuous clock helps to resolve several open questions in the literature: (1) the question of developing high-order schemes for Huyghebaert and De Raedt's approach, (2) the recently discussed problem of finding minimum gate implementation, and (3) a conjecture in deriving multiproduct formulas. We have also discussed how this overarching framework can be used for randomized quantum algorithms (qDrift in particular) and LCU-Taylor based algorithms. Numerically, our experiments also demonstrate the efficiency of high-order HDR algorithms for digitized adiabatic simulation, which is at least comparable as some Magnus-based algorithms.

ACKNOWLEDGMENTS

The authors were supported by NSFC Grant No. 12341104, the Shanghai Jiao Tong University 2030 Initiative, the Shanghai Science and Technology Innovation Action Plan (24LZ1401200), and the Fundamental Research Funds for the Central Universities. Y.C. was sponsored by Shanghai Pujiang Program (23PJ1404600). S.J. was also partially supported by the NSFC Grant No. 12426637. N.L. also acknowledges funding from the Science and Technology Commission of Shanghai Municipality (STCSM) Grant No. 24LZ1401200 (21JC1402900) and the NSFC Grant No. 12471411.

DATA AVAILABILITY

The data that support the findings of this article are not publicly available. The data are available from the authors upon reasonable request.

APPENDIX A: ADDITIONAL PROOFS

1. Proof of Theorem 3

The fidelity of ρ_ω with respect to the target state $|\psi(t)\rangle = \mathcal{U}(t,0)|\psi(0)\rangle$ is given as

$$\begin{aligned}\langle\psi(t)|\rho_\omega(t)|\psi(t)\rangle &= \int \mathrm{d}s\, |G(s-t)|^2\, \langle\psi(t)|\mathcal{U}(s,s-t)|\psi(0)\rangle\langle\psi(0)|\mathcal{U}(s,s-t)^\dagger|\psi(t)\rangle \\ &= \int \mathrm{d}s\, |G(s-t)|^2\, |\langle\psi(0)|\mathcal{U}(0,t)\mathcal{U}(s,s-t)|\psi(0)\rangle|^2 \\ &= \int \mathrm{d}s\, |G(s)|^2\, \underbrace{|\langle\psi(0)|\mathcal{U}(0,t)\mathcal{U}(s+t,s)|\psi(0)\rangle|^2}_{=:\theta(s)}.\end{aligned}$$

By Taylor's expansion of θ near $s \approx 0$,

$$\begin{aligned}\langle\psi(t)|\rho_\omega(t)|\psi(t)\rangle &= \int \mathrm{d}s\, |G(s)|^2 \sum_{\ell=0}^{\infty} \frac{\theta^{(\ell)}(0)}{\ell!} s^\ell \\ &= \sum_{\ell=0}^{\infty} \frac{\theta^{(\ell)}(0)}{\ell!} \left(\int \mathrm{d}s\, |G(s)|^2 s^\ell \right).\end{aligned}$$

Since we choose $|G|^2$ to be a Gaussian $\mathcal{N}(0,\omega^2)$, we have

$$\begin{aligned}\langle\psi(t)|\rho_\omega(t)|\psi(t)\rangle &= \sum_{\ell=0,2,4,\ldots} \frac{\theta^{(\ell)}(0)}{\ell!} \frac{2^{\ell/2}\Gamma(\ell+1/2)}{\sqrt{\pi}} \omega^\ell \\ &= 1 + \sum_{\ell=1,2,\ldots} \frac{\theta^{(2\ell)}(0)}{(2\ell)!} \frac{2^\ell \Gamma(\ell+1/2)}{\sqrt{\pi}} \omega^{2\ell}.\end{aligned}$$

The case $\theta^{(0)}(0) = 1$ is easy to verify by definition. By choosing various α_j and k_j that satisfy Eq. (15), we have

$$\begin{aligned}\langle\psi(t)|\sum_{j=1}^{M}\alpha_j\rho_{\omega/k_j}(t)|\psi(t)\rangle &= \sum_{j=1}^{M}\alpha_j\left(1+\sum_{\ell=1,2,\ldots}\frac{\theta^{(2\ell)}(0)}{(2\ell)!}\frac{2^\ell\Gamma(\ell+1/2)}{\sqrt{\pi}}\left(\frac{\omega}{k_j}\right)^{2\ell}\right)\\ &= 1+\sum_{\ell=1,2,\ldots}\frac{1}{(2\ell)!}\frac{2^\ell\Gamma(\ell+1/2)}{\sqrt{\pi}}\omega^{2\ell}\sum_{j=1}^{M}\alpha_j\left(\frac{1}{k_j}\right)^{2\ell}\theta^{(2\ell)}(0)\\ &= 1+\frac{\theta^{(2m)}(0)}{(2m)!}\frac{2^m\Gamma(m+1/2)}{\sqrt{\pi}}\omega^{2m}\sum_{j=1}^{M}\alpha_j\left(\frac{1}{k_j}\right)^{2m}+\mathcal{O}(\omega^{2m+2})\\ &= 1-C_m\omega^{2m}+\mathcal{O}(\omega^{2m+2}),\end{aligned}$$

where

$$C_m = -\frac{2^m\Gamma(m+1/2)}{(2m)!\sqrt{\pi}}\left(\sum_{j=1}^{M}\alpha_j\left(\frac{1}{k_j}\right)^{2m}\right)\theta^{(2\ell)}(0) > 0. \tag{A1}$$

Since $\rho_{\omega/k_j}(t)$ is a density matrix, it holds that $\langle\psi(t)|\sum_{j=1}^{M}\alpha_j\rho_{\omega/k_j}(t)|\psi(t)\rangle \leqslant 1$ is always true and thus $C_m \geqslant 0$. Then,

$$\begin{aligned}\left|\sum_{j=1}^{M}\alpha_j\mathrm{tr}(\widehat{O}\rho_{\omega/k_j}(t)) - \mathrm{tr}(\widehat{O}|\psi(t)\rangle\langle\psi(t)|)\right| &\leqslant \left\|\sum_{j=1}^{M}\alpha_j\rho_{\omega/k_j}(t) - |\psi(t)\rangle\langle\psi(t)|\right\|_1\\ &\leqslant 2\sqrt{1-\langle\psi(t)|\sum_{j=1}^{M}\alpha_j\rho_{\omega/k_j}(t)|\psi(t)\rangle}\\ &= 2\sqrt{C_m}\,\omega^m+\mathcal{O}(\omega^{m+2}).\end{aligned}$$

2. Proof of Theorem 4

Recall from the error estimates in Ref. [33, Lemma 11] that

$$\||\psi(1)\rangle\langle\psi(1)| - \mathrm{tr}_s(|\Psi(t)\rangle\langle\Psi(t)|)\|_{\mathrm{tr}} \leqslant \sqrt{C}\omega.$$

By the triangle inequality of trace norm, one needs

$$\sqrt{C}\omega \leqslant \sqrt{\epsilon}. \tag{A2}$$

By Ref. [33, Lemma 11], the constant C is

$$\begin{aligned}C &= \langle H^2(1)\rangle - 2\mathrm{Re}(\langle\psi(1)|H(1)\mathcal{U}(t,0)H(0)|\psi(0)\rangle) + \langle H^2(0)\rangle - (\langle H(1)\rangle - \langle H(0)\rangle)^2\\ &= \langle H^2(1)\rangle - 2T\lambda_1\langle H(1)\rangle + T^2\lambda_1^2 - \langle H(1)\rangle^2 + 2T\lambda_1\langle H(1)\rangle - T^2\lambda_1^2\\ &= \langle H^2(1)\rangle - \langle H(1)\rangle^2,\end{aligned}$$

where $\langle O(t)\rangle := \langle\psi(t)|O(t)|\psi(t)\rangle$ for any time-dependent observable O and time $t \in [0,1]$. To get the above, we have used the fact that the state $\psi(0)$ is prepared as a ground state of $\boldsymbol{h}_1$ [with $\boldsymbol{h}_1|\psi(0)\rangle = \lambda_1|\psi(0)\rangle$ and thus $H(0)|\psi(0)\rangle = T\lambda_1|\psi(0)\rangle$].

Suppose that $|\psi(1)\rangle = \alpha|\varphi_{\mathrm{true}}\rangle + \beta|\varphi_\perp\rangle$, where $|\varphi_\perp\rangle$ is perpendicular to $|\varphi_{\mathrm{true}}\rangle$. By the error assumption in Eq. (13), and normalization of $|\psi(1)\rangle$,

$$\alpha = 1-\mathcal{O}(\epsilon), \quad \beta = \mathcal{O}(\sqrt{\epsilon}).$$

With such a decomposition, one can compute that

$$\begin{aligned}\langle H^2(1)\rangle &= T^2\langle\alpha\varphi_{\mathrm{true}}+\beta\varphi_\perp|\boldsymbol{h}_2^2|\alpha\varphi_{\mathrm{true}}+\beta\varphi_\perp\rangle\\ &= T^2\big(|\alpha|^2\lambda_2^2+|\beta|^2\langle\varphi_\perp|\boldsymbol{h}_2^2|\varphi_\perp\rangle\big),\\ \langle H(1)\rangle &= T\langle\alpha\varphi_{\mathrm{true}}+\beta\varphi_\perp|\boldsymbol{h}_2|\alpha\varphi_{\mathrm{true}}+\beta\varphi_\perp\rangle\\ &= T(|\alpha|^2\lambda_2+|\beta|^2\langle\varphi_\perp|\boldsymbol{h}_2|\varphi_\perp\rangle),\end{aligned}$$

where λ_2 is the ground energy of $\boldsymbol{h}_2$ and $\boldsymbol{h}_2|\varphi_{\text{true}}\rangle = \lambda_2|\varphi_{\text{true}}\rangle$. Hence,

$$\begin{aligned}\frac{1}{T^2}(\langle H^2(1)\rangle - \langle H(1)\rangle^2) &= (|\alpha|^2 - |\alpha|^4)\lambda_2^2 + |\beta|^2\langle\varphi_\perp|\boldsymbol{h}_2^2|\varphi_\perp\rangle - |\beta|^4\langle\varphi_\perp|\boldsymbol{h}_2|\varphi_\perp\rangle^2 - 2|\alpha|^2|\beta|^2\lambda_2\langle\varphi_\perp|\boldsymbol{h}_2|\varphi_\perp\rangle \\ &= \mathcal{O}\big(\epsilon\lambda_2^2 + \epsilon\langle\varphi_\perp|\boldsymbol{h}_2^2|\varphi_\perp\rangle + \epsilon^2\langle\varphi_\perp|\boldsymbol{h}_2|\varphi_\perp\rangle^2 + \epsilon\lambda_2\langle\varphi_\perp|\boldsymbol{h}_2|\varphi_\perp\rangle\big) \\ &= \mathcal{O}\big(\epsilon\big(\lambda_2^2 + \|\boldsymbol{h}_2\|^2\big) + \epsilon^2\|\boldsymbol{h}_2\|^2\big) \\ &= \mathcal{O}(\epsilon\|\boldsymbol{h}_2\|^2).\end{aligned}$$

To maintain the same order of error, it is sufficient to pick

$$\sqrt{C}\omega = \mathcal{O}(T\sqrt{\epsilon}\|\boldsymbol{h}_2\|\omega) \leqslant \sqrt{\epsilon},$$

which leads to Eq. (17).

3. Proof of Lemma 7

We list without proof some facts, which can be easily validated by definition:

Lemma 15. If the quantum state $|\Psi\rangle$ comes from the augmented space $\mathscr{X}$, then for any $s' \in \mathbb{T}$, $\tau \in \mathbb{R}$, any index k and $\varphi \in \mathcal{H}$, we have

$$\begin{aligned}&\langle s'|\langle\varphi|e^{-i\tau H_k(\hat{s})}|\Psi\rangle = \langle\varphi|e^{-i\tau H_k(s')}|\Psi(s',\cdot)\rangle = \langle s'|\langle\varphi|\mathbf{I}\otimes e^{-i\tau H_k(s')}|\Psi\rangle, \\ &\langle s'|\langle\varphi|e^{-i\tau\hat{p}_s\otimes\mathbf{I}}|\Psi\rangle = \langle s'-\tau|\langle\varphi|\Psi\rangle \equiv \langle\varphi|\Psi(s'-\tau,\cdot)\rangle.\end{aligned} \tag{A3}$$

Next, we shall prove the first equation in Lemma 7 (also copied below):

$$\langle s'|\langle\varphi|\prod_{k=1}^{\Lambda+1} e^{A_k\theta\Delta t}|\Psi\rangle = \langle s'-\theta\Delta t|\langle\varphi|(\mathbf{I}\otimes U_F(s',s'-\theta\Delta t))|\Psi\rangle,$$

and the second one can be similarly validated.

$$\begin{aligned}\langle s'|\langle\varphi|\prod_{k=1}^{\Lambda+1} e^{A_k\theta\Delta t}|\Psi\rangle &= \langle s'|\langle\varphi|\prod_{k=1}^{\Lambda'} e^{-i\theta\Delta t H_k(\hat{s})}e^{-i\theta\Delta t\hat{p}_s\otimes\mathbf{I}}\prod_{k=\Lambda'+1}^{\Lambda} e^{-i\theta\Delta t H_k(\hat{s})}|\Psi\rangle \\ &\overset{(A3)}{=} \langle s'|\left(\langle\varphi|\prod_{k=1}^{\Lambda'} e^{-i\theta\Delta t H_k(s')}\right)e^{-i\theta\Delta t\hat{p}_s\otimes\mathbf{I}}\prod_{k=\Lambda'+1}^{\Lambda} e^{-i\theta\Delta t H_k(\hat{s})}|\Psi\rangle \\ &\overset{(A3)}{=} \langle s'-\theta\Delta t|\left(\langle\varphi|\prod_{k=1}^{\Lambda'} e^{-i\theta\Delta t H_k(s')}\right)\prod_{k=\Lambda'+1}^{\Lambda} e^{-i\theta\Delta t H_k(\hat{s})}|\Psi\rangle \\ &\overset{(A3)}{=} \langle s'-\theta\Delta t|\left(\langle\varphi|\prod_{k=1}^{\Lambda'} e^{-i\theta\Delta t H_k(s')}\prod_{k=\Lambda'+1}^{\Lambda} e^{-i\theta\Delta t H_k(s'-\theta\Delta t)}\right)|\Psi\rangle \\ &= \left(\langle\varphi|\prod_{k=1}^{\Lambda'} e^{-i\theta\Delta t H_k(s')}\prod_{k=\Lambda'+1}^{\Lambda} e^{-i\theta\Delta t H_k(s'-\theta\Delta t)}\right)|\Psi(s'-\theta\Delta t,\cdot)\rangle \\ &= \langle s'-\theta\Delta t|\langle\varphi|(\mathbf{I}\otimes U_F(s',s'-\theta\Delta t))|\Psi\rangle.\end{aligned}$$

Thus, the proof is complete.

4. Explicit form of the HDR scheme with the FRS weight

When one applies the Forest-Ruth-Suzki's formula to HDR scheme, one has

$$\begin{aligned}\mathcal{T}e^{-i\int_t^{t+\Delta t} H_1(s)+H_2(s)\,\mathrm{d}s} \approx{}& \widetilde{U}_F\left(t+\Delta t, t+\left(1-\frac{\gamma}{2}\right)\Delta t\right)\widetilde{U}_B\left(t+\left(1-\frac{\gamma}{2}\right)\Delta t, t+(1-\gamma)\Delta t\right) \\ &\times\widetilde{U}_F\left(t+(1-\gamma)\Delta t, t+\frac{1}{2}\Delta t\right)\widetilde{U}_B\left(t+\frac{1}{2}\Delta t, t+\gamma\Delta t\right)\widetilde{U}_F\left(t+\gamma\Delta t, t+\frac{\gamma}{2}\Delta t\right)\widetilde{U}_B\left(t+\frac{\gamma}{2}\Delta t, t\right)\end{aligned}$$

$$= e_{\mathcal{T}}^{-i\int_{(1-\frac{\gamma}{2})\Delta t}^{\Delta t} H_1(t+r)\,\mathrm{d}r} e_{\mathcal{T}}^{-i\int_{(1-\gamma)\Delta t}^{\Delta t} H_2(t+r)\,\mathrm{d}r} e_{\mathcal{T}}^{-i\int_{\frac{1}{2}\Delta t}^{(1-\frac{\gamma}{2})\Delta t} H_1(t+r)\mathrm{d}r} e_{\mathcal{T}}^{-i\int_{\gamma\Delta t}^{(1-\gamma)\Delta t} H_2(t+r)\mathrm{d}r}$$
$$\times e_{\mathcal{T}}^{-i\int_{\frac{\gamma}{2}\Delta t}^{\frac{1}{2}\Delta t} H_1(t+r)\mathrm{d}r} e_{\mathcal{T}}^{-i\int_{0}^{\gamma\Delta t} H_2(t+r)\mathrm{d}r} e_{\mathcal{T}}^{-i\int_{0}^{\frac{\gamma}{2}\Delta t} H_1(t+r)\mathrm{d}r}. \tag{A4}$$

5. Proofs for Sec. VII

Proof of Lemma 11. We shall prove the following result: for any density matrix ρ,

$$e^{-i\Delta t H}\rho\, e^{i\Delta t H} - \int \mathrm{d}\omega\, \lambda(\omega) e^{-i\Delta t H_\omega}\, \rho\, e^{i\Delta t H_\omega} = -\frac{\Delta t^2}{2}\iint \mathrm{d}\omega_1 \mathrm{d}\omega_2\, \lambda(\omega_1)(\lambda(\omega_2) - \delta(\omega_1-\omega_2))\big[H_{\omega_1}, \big[H_{\omega_2}, \rho\big]\big] + \mathcal{O}(\Delta t^3). \tag{A5}$$

The conclusion of lemma can be readily obtained by applying the triangle inequality to this equation.

One can prove the last equation by direct expansion:

$$\begin{aligned}
&e^{-i\Delta t H}\rho\, e^{i\Delta t H} - \int \mathrm{d}\omega\, \lambda(\omega) e^{-i\Delta t H_\omega}\, \rho\, e^{i\Delta t H_\omega} \\
&= \Delta t^2\left(-\frac{1}{2}[H,[H,\rho]] + \frac{1}{2}\int \mathrm{d}\omega\, \lambda(\omega)[H_\omega,[H_\omega,\rho]]\right) + \mathcal{O}(\Delta t^3) \\
&= -\frac{1}{2}\Delta t^2\left(\iint \mathrm{d}\omega_1 \mathrm{d}\omega_2\, \lambda(\omega_1)\lambda(\omega_2)\big[H_{\omega_1}, \big[H_{\omega_2}, \rho\big]\big] - \int \mathrm{d}\omega\, \lambda(\omega)\big[H_\omega, \big[H_\omega, \rho\big]\big]\right) + \mathcal{O}(\Delta t^3) \\
&= -\frac{1}{2}\Delta t^2\left(\iint \mathrm{d}\omega_1 \mathrm{d}\omega_2\, \lambda(\omega_1)(\lambda(\omega_2) - \delta(\omega_1-\omega_2))\, \big[H_{\omega_1}, \big[H_{\omega_2}, \rho\big]\big]\right) + \mathcal{O}(\Delta t^3).
\end{aligned}$$

■

Proof of Lemma 12. As can be seen, the only error comes from the application of time-independent qDrift algorithm; thus, by the proof of Lemma 11 or more specifically by Eq. (A5),

$$\begin{aligned}
\mathcal{U}(t+\Delta t,t)\rho\mathcal{U}(t+\Delta t,t)^\dagger - \mathcal{E}_{\lambda,t,\Delta t}(\rho) &= \langle t+\Delta t|_s\left(-\frac{1}{2}\Delta t^2 \sum_{k_1,k_2}\lambda_{k_1}\big(\lambda_{k_2} - \delta_{k_1,k_2}\big)\big[\widetilde{H}_{k_1}, \big[\widetilde{H}_{k_2}, |\mathbb{1}\rangle\langle\mathbb{1}|\otimes\rho\big]\big]\right)|t+\Delta t\rangle_s + \mathcal{O}(\Delta t^3) \\
&= -\frac{1}{2}\Delta t^2 \sum_{k_1,k_2}\lambda_{k_1}\big(\lambda_{k_2} - \delta_{k_1,k_2}\big)\langle t+\Delta t|_s\big[\widetilde{H}_{k_1}, \big[\widetilde{H}_{k_2}, |\mathbb{1}\rangle\langle\mathbb{1}|\otimes\rho\big]\big]|t+\Delta t\rangle_s + \mathcal{O}(\Delta t^3).
\end{aligned}$$

Next, let us estimate

$$\begin{aligned}
\big[\widetilde{H}_{k_1}, \big[\widetilde{H}_{k_2}, |\mathbb{1}\rangle\langle\mathbb{1}|\otimes\rho\big]\big] &= \left[\hat{p}_s\otimes\mathbf{I} + \frac{H_{k_1}(\hat{s})}{\lambda_{k_1}}, \left[\hat{p}_s\otimes\mathbf{I} + \frac{H_{k_2}(\hat{s})}{\lambda_{k_2}}, |\mathbb{1}\rangle\langle\mathbb{1}|\otimes\rho\right]\right] \\
&= \frac{1}{\lambda_{k_2}}\left[\hat{p}_s\otimes\mathbf{I} + \frac{H_{k_1}(\hat{s})}{\lambda_{k_1}}, \big|f_{k_2}(s)\big\rangle\langle\mathbb{1}|\otimes\boldsymbol{h}_2\rho - |\mathbb{1}\rangle\big\langle f_{k_2}(s)\big|\otimes\rho\boldsymbol{h}_2\right] \\
&= \frac{1}{\lambda_{k_2}}\begin{pmatrix} -i\big|f'_{k_2}(s)\big\rangle\langle\mathbb{1}|\otimes\boldsymbol{h}_2\rho + \frac{1}{\lambda_{k_1}}\big|f_{k_1}(s)f_{k_2}(s)\big\rangle\langle\mathbb{1}|\otimes\boldsymbol{h}_1\boldsymbol{h}_2\rho \\ \frac{1}{\lambda_{k_1}}\big|f_{k_2}(s)\big\rangle\big\langle f_{k_1}(s)\big|\otimes\boldsymbol{h}_2\rho\boldsymbol{h}_1 + |\mathbb{1}\rangle\big\langle(-i)f'_{k_2}(s)\big|\otimes\rho\boldsymbol{h}_2 \\ -\frac{1}{\lambda_{k_1}}\big|f_{k_1}(s)\big\rangle\big\langle f_{k_2}(s)\big|\otimes\boldsymbol{h}_1\rho\boldsymbol{h}_2 + \frac{1}{\lambda_{k_1}}|\mathbb{1}\rangle\big\langle f_{k_2}(s)f_{k_1}(s)\big|\otimes\rho\boldsymbol{h}_2\boldsymbol{h}_1 \end{pmatrix},
\end{aligned}$$

where the notation $|f_k(s)\rangle \equiv \int \mathrm{d}s\, f_k(s)|s\rangle$ and similar conventions apply to other places. Given such an expansion, and with expressions (2) and (3), one can straightforwardly validate that

$$\begin{aligned}
&\mathcal{U}(t+\Delta t,t)\rho\mathcal{U}(t+\Delta t,t)^\dagger - \mathcal{E}_{\lambda,t,\Delta t}(\rho) \\
&= -\frac{\Delta t^2}{2}\sum_{k_1,k_2}\lambda_{k_1}\big(\lambda_{k_2} - \delta_{k_1,k_2}\big)\left(\frac{-if'_{k_2}(t+\Delta t)}{\lambda_{k_2}}\big[\boldsymbol{h}_{k_2},\rho\big] + \frac{f_{k_1}(t+\Delta t)f_{k_2}(t+\Delta t)}{\lambda_{k_1}\lambda_{k_2}}\big[\boldsymbol{h}_{k_1},\big[\boldsymbol{h}_{k_2},\rho\big]\big]\right) + \mathcal{O}(\Delta t^3) \\
&= -\frac{\Delta t^2}{2}\sum_{k_1,k_2}\lambda_{k_1}\big(\lambda_{k_2} - \delta_{k_1,k_2}\big)\frac{f_{k_1}(t+\Delta t)f_{k_2}(t+\Delta t)}{\lambda_{k_1}\lambda_{k_2}}\big[\boldsymbol{h}_{k_1},\big[\boldsymbol{h}_{k_2},\rho\big]\big] + \mathcal{O}(\Delta t^3).
\end{aligned}$$

The third line is obtained by observing that $\sum_{k_1}\lambda_{k_1}(\lambda_{k_2}-\delta_{k_1,k_2})=\lambda_{k_2}-\lambda_{k_2}=0$. Finally, by applying the triangle inequality, one can immediately obtain the conclusion. ■

Proof of Lemma 13. The proof is not much different from Lemma 12. We can similarly verify that for $\omega_1=(k_1,r_1)$, $\omega_2=(k_2,r_2)$, by Lemma 11, or more specifically by Eq. (A5), the error term is

$$\begin{aligned}
&\mathcal{U}(t+\Delta t,t)\,\rho\,\mathcal{U}(t+\Delta t,t)^\dagger-\mathcal{E}_{\mu,t,\Delta t}(\rho)\\
&\quad=-\frac{\Delta t^2}{2}\iint \mathrm{d}\omega_1\mathrm{d}\omega_2\;\mu(\omega_1)(\mu(\omega_2)-\delta(\omega_1-\omega_2))\left(\frac{-if_{k_2}'(t+\Delta t)}{\mu(\omega_2)}\big[\boldsymbol{h}_{k_2},\rho\big]+\frac{f_{k_1}(t+\Delta t)f_{k_2}(t+\Delta t)}{\mu(\omega_1)\mu(\omega_2)}\big[\boldsymbol{h}_{k_1},\big[\boldsymbol{h}_{k_2},\rho\big]\big]\right)\\
&\qquad+\mathcal{O}(\Delta t^3)\\
&\quad=-\frac{\Delta t^2}{2}\iint \mathrm{d}\omega_1\mathrm{d}\omega_2\;\mu(\omega_1)(\mu(\omega_2)-\delta(\omega_1-\omega_2))\left(\frac{f_{k_1}(t+\Delta t)f_{k_2}(t+\Delta t)}{\mu(\omega_1)\mu(\omega_2)}[\boldsymbol{h}_{k_1},[\boldsymbol{h}_{k_2},\rho]]\right)+\mathcal{O}(\Delta t^3).
\end{aligned}$$

Finally, one can easily get the upper bound of C via the triangle inequality. ■

Proof of Lemma 14. As we choose Hamiltonians with the form in Eqs. (2) and (3),

$$\begin{aligned}
\mathcal{E}_{\mu,t,\Delta t}(\rho)&\overset{(37)}{=}\sum_k\int_0^1\mathrm{d}r\;\mu(k,r)\,e^{-i\frac{\int_t^{t+\Delta t}H_k(s)\mathrm{d}s}{\mu(k,r)}}\,\rho\,e^{i\frac{\int_t^{t+\Delta t}H_k(s)\mathrm{d}s}{\mu(k,r)}}\\
&=\sum_k\int_0^1\mathrm{d}r\;\mu(k,r)\,e^{-i\Delta t\frac{\frac{1}{\Delta t}\int_t^{t+\Delta t}f_k(s)\mathrm{d}s}{\mu(k,r)}\boldsymbol{h}_k}\,\rho\,e^{i\Delta t\frac{\frac{1}{\Delta t}\int_t^{t+\Delta t}f_k(s)\mathrm{d}s}{\mu(k,r)}\boldsymbol{h}_k}.
\end{aligned}$$

For each k, define $F_k:[0,1]\to\mathbb{R}^+$ and $\tau_k:[0,1]\to[0,1]$ by

$$F_k(r)=\int_0^r f_k(t+\Delta t s)\,\mathrm{d}s,\qquad \tau_k(r):=F_k^{-1}(F_k(1)r). \tag{A6}$$

It is easy to verify that F_k and τ_k are strictly monotone increasing. Let us further define a hybrid probability measure q via

$$q(k,\tau_k(r)):=\frac{\mu(k,r)f_k(t+\Delta t\tau_k(r))}{F_k(1)}. \tag{A7}$$

Then, it is easy to verify that

$$\begin{aligned}
q(k,\tau_k(r))\tau_k'(r)&=\frac{\mu(k,r)f_k(t+\Delta t\tau_k(r))}{F_k(1)}\tau_k'(r)\\
&=\frac{\mu(k,r)f_k(t+\Delta t\tau_k(r))}{F_k(1)}\frac{F_k(1)}{F_k'\big(F_k^{-1}(F_k(1)r)\big)}\\
&=\frac{\mu(k,r)f_k(t+\Delta t\tau_k(r))}{f_k\big(t+\Delta tF_k^{-1}(F_k(1)r)\big)}\overset{(A6)}{=}\mu(k,r).
\end{aligned}$$

Therefore, by change of variables,

$$\begin{aligned}
\mathcal{E}_{\mu,t,\Delta t}(\rho)&=\sum_k\int_0^1\mathrm{d}r\;\mu(k,r)\,e^{-i\Delta t\frac{F_k(1)}{\mu(k,r)}\boldsymbol{h}_k}\,\rho\,e^{i\Delta t\frac{F_k(1)}{\mu(k,r)}\boldsymbol{h}_k}\\
&=\sum_k\int_0^1\mathrm{d}\tau_k\;q(k,\tau_k)e^{-i\Delta t\frac{F_k(1)f_k(t+\Delta t\tau_k)}{\mu(k,r)f_k(t+\Delta t\tau_k)}\boldsymbol{h}_k}\rho e^{i\Delta t\frac{F_k(1)f_k(t+\Delta t\tau_k)}{\mu(k,r)f_k(t+\Delta t\tau_k)}\boldsymbol{h}_k}\\
&\overset{(A7)}{=}\sum_k\int_0^1\mathrm{d}\tau_k\;q(k,\tau_k)e^{-i\Delta t\frac{f_k(t+\Delta t\tau_k)}{q(k,\tau_k)}\boldsymbol{h}_k}\rho e^{i\Delta t\frac{f_k(t+\Delta t\tau_k)}{q(k,\tau_k)}\boldsymbol{h}_k}\\
&\overset{(3)}{=}\sum_k\int_0^1\mathrm{d}\tau_k\;q(k,\tau_k)e^{-i\Delta t\frac{H_k(t+\Delta t\tau_k)}{q(k,\tau_k)}}\rho e^{i\Delta t\frac{H_k(t+\Delta t\tau_k)}{q(k,\tau_k)}}.
\end{aligned}$$

Finally, by removing the subscript k in τ for simplicity of notations,

$$\mathcal{E}_{\mu,t,\Delta t}(\rho)=\sum_k\int_0^1\mathrm{d}\tau\;q(k,\tau)e^{-i\Delta t\frac{H_k(t+\Delta t\tau)}{q(k,\tau)}}\;\rho\;e^{i\Delta t\frac{H_k(t+\Delta t\tau)}{q(k,\tau)}}\overset{(38)}{=}\mathcal{E}^{(\text{c-qDrift})}_{q,t,\Delta t}(\rho).$$

■

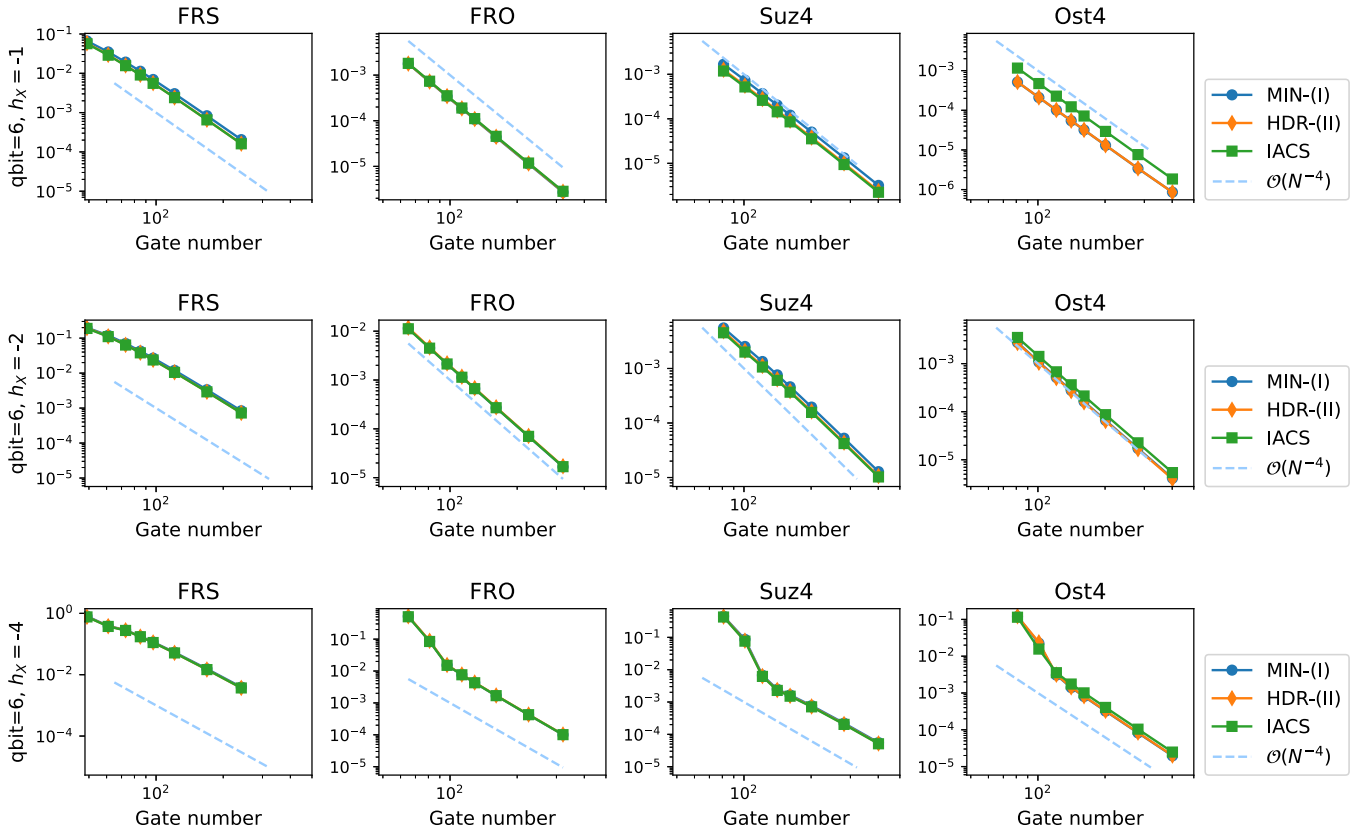


FIG. 3. Averaged simulation error in trace distance for the quantum Ising model with respect to the gate counts N for various time-dependent schemes. "MIN-(I)" refers to the scheme (23) with the ordering H_1, $\hat{p}$, and H_2. HDR refers to the scheme in Eq. (29). IACS refers to the scheme in Ref. [27]; see also Eq. (26). The blue dashed line indicates the scaling $\mathcal{O}(N^{-4})$ and is the same for all subplots.

APPENDIX B: SUPPLEMENTARY DETAILS FOR NUMERICAL EXPERIMENTS

1. Weights for time-independent splitting schemes

All the following weights for fourth-order splitting schemes come from a summary in Ref. [66]:

(i) Forest-Ruth-Suzuki [66, Sec. 3.2.3] refers to the splitting scheme in Eq. (21) with cycle $q = 3$, where

$$a_1 = \frac{\gamma}{2}, \quad b_1 = \gamma, \quad a_2 = \frac{1-\gamma}{2}, \quad b_2 = 1 - 2\gamma,$$
$$a_3 = a_2, \quad b_3 = b_1, \quad a_4 = a_1,$$

and $\gamma = (2 - 2^{1/3})^{-1} \approx 1.351\,207\,191\,959\,6578$.

(ii) Omelyan's Forest-Ruth-type (FRO) [66, Sec. 3.2.4] refers to the splitting scheme in Eq. (21) with cycle $q = 4$, where

$$\begin{aligned} a_1 &= 0.172\,086\,559\,029\,5143, & b_1 &= 0.591\,562\,030\,755\,1568,\\ a_2 &= -0.161\,621\,762\,210\,7222, & b_2 &= 1/2 - b_1,\\ a_3 &= 1 - 2(a_1 + a_2), & b_3 &= b_2,\\ a_4 &= a_2, & b_4 &= b_1,\\ a_5 &= a_1. \end{aligned}$$

(iii) Suzuki's fourth-order scheme (Suz4) [66, Sec. 3.2.7] refers to the splitting scheme in Eq. (21) with cycle $q = 5$, where

$$\begin{aligned} a_1 &= 0.207\,245\,385\,897\,1879, & b_1 &= 0.414\,490\,771\,794\,3757,\\ a_2 &= 0.414\,490\,771\,794\,3757, & b_2 &= 0.414\,490\,771\,794\,3757,\\ a_3 &= 1/2 - (a_1 + a_2), & b_3 &= 1 - 2(b_1 + b_2),\\ a_4 &= 1/2 - (a_1 + a_2), & b_4 &= b_2,\\ a_5 &= a_2, & b_5 &= b_1,\\ a_6 &= a_1. \end{aligned}$$

(iv) Ostmeyer's optimized 4th order (Ost4) [66, Sec. 3.2.8] refers to the splitting scheme in Eq. (21) with cycle $q = 5$, where

$$\begin{aligned} a_1 &= 0.092\,575\,474\,731\,957\,87, & b_1 &= 0.254\,099\,631\,552\,9392,\\ a_2 &= 0.462\,716\,031\,021\,0738, & b_2 &= -0.167\,651\,724\,011\,9692,\\ a_3 &= 1/2 - (a_1 + a_2), & b_3 &= 1 - 2(b_1 + b_2),\\ a_4 &= 1/2 - (a_1 + a_2), & b_4 &= b_2,\\ a_5 &= a_2, & b_5 &= b_1,\\ a_6 &= a_1. \end{aligned}$$

2. The quantum Ising chain

We also consider the same problem in Ref. [27, Sec. 5] for $H(t) = f_1(t)\boldsymbol{h}_1 + f_2(t)\boldsymbol{h}_2$, where

$$\boldsymbol{h}_1 = \sum_{j=1}^{L} h_X \sigma_X^{(j)}, \quad \boldsymbol{h}_2 = \sum_{j=1}^{L} J\sigma_Z^{(j)} \otimes \sigma_Z^{(j+1)} + h_Z \sigma_Z^{(j)}, \quad f_1(t) = \pi \sin(\pi t), \quad f_2(t) = \pi,$$

and $J = -1$, $h_Z = 0.2$. The periodic boundary condition is imposed for the 1D Ising chain, and $\sigma_{X,Y,Z}^{(j)}$ denotes the Pauli matrices for the site j. It can be easily verified that the maximally entangled state $|+\rangle^{\otimes L}$ is the ground state of $\boldsymbol{h}_1$ and we will use it as the initial condition. We consider $L = 6$ qubits, and various $h_X = -1, -2, -4$. We notice from Fig. 3 that when the magnitude of h_X is smaller, the performance of Eq. (29) is slightly better than IACS; overall, it is almost indistinguishable from IACS scheme for this example.

[1] R. P. Feynman, Simulating physics with computers, Int. J. Theor. Phys. **21**, 467 (1982).

[2] S. Lloyd, Universal quantum simulators, Science **273**, 1073 (1996).

[3] H. F. Trotter, On the product of semi-groups of operators, Proc. Am. Math. Soc. **10**, 545 (1959).

[4] M. Suzuki, Generalized Trotter's formula and systematic approximants of exponential operators and inner derivations with applications to many-body problems, Commun. Math. Phys. **51**, 183 (1976).

[5] M. Suzuki, Fractal decomposition of exponential operators with applications to many-body theories and Monte Carlo simulations, Phys. Lett. A **146**, 319 (1990).

[6] M. Suzuki, General theory of fractal path integrals with applications to many-body theories and statistical physics, J. Math. Phys. **32**, 400 (1991).

[7] S. A. Chin and J. Geiser, Multi-product operator splitting as a general method of solving autonomous and nonautonomous equations, IMA J. Numer. Anal. **31**, 1552 (2011).

[8] A. M. Childs and N. Wiebe, Hamiltonian simulation using linear combinations of unitary operations, Quantum Inf. Comput. **12**, 901 (2012).

[9] G. H. Low, V. Kliuchnikov, and N. Wiebe, Well-conditioned multiproduct Hamiltonian simulation, arXiv:1907.11679.

[10] S. Endo, Q. Zhao, Y. Li, S. Benjamin, and X. Yuan, Mitigating algorithmic errors in a Hamiltonian simulation, Phys. Rev. A **99**, 012334 (2019).

[11] D. Poulin, A. Qarry, R. Somma, and F. Verstraete, Quantum simulation of time-dependent Hamiltonians and the convenient illusion of Hilbert space, Phys. Rev. Lett. **106**, 170501 (2011).

[12] C. Zhang, Randomized algorithms for Hamiltonian simulation, in *Monte Carlo and Quasi-Monte Carlo Methods 2010*, edited by L. Plaskota and H. Woźniakowski (Springer, Berlin, 2012), pp. 709–719.

[13] A. M. Childs, A. Ostrander, and Y. Su, Faster quantum simulation by randomization, Quantum **3**, 182 (2019).

[14] E. Campbell, Random compiler for fast Hamiltonian simulation, Phys. Rev. Lett. **123**, 070503 (2019).

[15] D. W. Berry, A. M. Childs, R. Cleve, R. Kothari, and R. D. Somma, Simulating Hamiltonian dynamics with a truncated Taylor series, Phys. Rev. Lett. **114**, 090502 (2015).

[16] G. H. Low and I. L. Chuang, Hamiltonian simulation by qubitization, Quantum **3**, 163 (2019).

[17] J. L. Bosse, A. M. Childs, C. Derby, F. M. Gambetta, A. Montanaro, and R. A. Santos, Efficient and practical Hamiltonian simulation from time-dependent product formulas, Nat. Commun. **16**, 2673 (2025).

[18] K. Sharma and M. C. Tran, Hamiltonian simulation in the interaction picture using the Magnus expansion, arXiv:2404.02966.

[19] M. Suzuki, Hybrid exponential product formulas for unbounded operators with possible applications to Monte Carlo simulations, Phys. Lett. A **201**, 425 (1995).

[20] J. Huyghebaert and H. D. Raedt, Product formula methods for time-dependent Schrodinger problems, J. Phys. A: Math. Gen. **23**, 5777 (1990).

[21] M. Suzuki, General decomposition theory of ordered exponentials, Proc. Jpn. Acad. Ser. B **69**, 161 (1993).

[22] S. Blanes, F. Casas, J. A. Oteo, and J. Ros, The Magnus expansion and some of its applications, Phys. Rep. **470**, 151 (2009).

[23] J. Watkins, N. Wiebe, A. Roggero, and D. Lee, Time-dependent Hamiltonian simulation using discrete-clock constructions, PRX Quantum **5**, 040316 (2024).

[24] K. Mizuta and K. Fujii, Optimal Hamiltonian simulation for time-periodic systems, Quantum **7**, 962 (2023).

[25] K. Mizuta, Optimal and nearly optimal simulation of multiperiodic time-dependent Hamiltonians, Phys. Rev. Res. **5**, 033067 (2023).

[26] D. W. Berry, A. M. Childs, Y. Su, X. Wang, and N. Wiebe, Time-dependent Hamiltonian simulation with L^1-norm scaling, Quantum **4**, 254 (2020).

[27] T. N. Ikeda, A. Abrar, I. L. Chuang, and S. Sugiura, Minimum Trotterization formulas for a time-dependent Hamiltonian, Quantum **7**, 1168 (2023).

[28] T. Albash and D. A. Lidar, Adiabatic quantum computation, Rev. Mod. Phys. **90**, 015002 (2018).

[29] G. H. Low and N. Wiebe, Hamiltonian simulation in the interaction picture, arXiv:1805.00675.

[30] S. Jin, N. Liu, and Y. Yu, Quantum simulation of partial differential equations via Schrödingerization, Phys. Rev. Lett. **133**, 230602 (2024).

[31] S. Jin, N. Liu, and Y. Yu, Quantum simulation of partial differential equations: Applications and detailed analysis, Phys. Rev. A **108**, 032603 (2023).

[32] S. Jin and N. Liu, Analog quantum simulation of partial differential equations, Quantum Sci. Technol. **9**, 035047 (2024).

[33] Y. Cao, S. Jin, and N. Liu, Quantum simulation for time-dependent Hamiltonians—with applications to non-autonomous ordinary and partial differential equations, J. Phys. A: Math. Theor. **58**, 155304 (2025).

[34] D. W. Berry, G. Ahokas, R. Cleve, and B. C. Sanders, Efficient quantum algorithms for simulating sparse Hamiltonians, Commun. Math. Phys. **270**, 359 (2007).

[35] H. Sambe, Steady states and quasienergies of a quantum-mechanical system in an oscillating field, Phys. Rev. A **7**, 2203 (1973).

[36] J. S. Howland, Stationary scattering theory for time-dependent Hamiltonians, Math. Ann. **207**, 315 (1974).

[37] U. Peskin and N. Moiseyev, The solution of the time-dependent Schrödinger equation by the (t, t') method: Theory, computational algorithm and applications, J. Chem. Phys. **99**, 4590 (1993).

[38] D. Burgarth, P. Facchi, and R. Hillier, Control of quantum noise: On the role of dilations, Ann. Henri Poincaré **24**, 325 (2023).

[39] M. Reed and B. Simon, *Methods of Mathematical Physics. Fourier Analysis, Self-Adjointness* (Academic Press, San Diego, CA, 1975).

[40] J. R. McClean, J. A. Parkhill, and A. Aspuru-Guzik, Feynman's clock, a new variational principle, and parallel-in-time quantum dynamics, Proc. Natl. Acad. Sci. USA **110**, E3901 (2013).

[41] A. Miessen, P. J. Ollitrault, F. Tacchino, and I. Tavernelli, Quantum algorithms for quantum dynamics, Nat. Comput. Sci. **3**, 25 (2023).

[42] H. De Raedt, Product formula algorithms for solving the time dependent Schrödinger equation, Comput. Phys. Rep. **7**, 1 (1987).

[43] A. M. Childs, Y. Su, M. C. Tran, N. Wiebe, and S. Zhu, Theory of Trotter error with commutator scaling, Phys. Rev. X **11**, 011020 (2021).

[44] N. Hatano and M. Suzuki, Finding exponential product formulas of higher orders, in *Quantum Annealing and Other Optimization Methods*, edited by A. Das and B. K. Chakrabarti (Springer, Berlin, 2005), pp. 37–68.

[45] N. Wiebe, D. Berry, P. Høyer, and B. C. Sanders, Higher order decompositions of ordered operator exponentials, J. Phys. A: Math. Theor. **43**, 065203 (2010).

[46] N. Wiebe, D. W. Berry, P. Høyer, and B. C. Sanders, Simulating quantum dynamics on a quantum computer, J. Phys. A: Math. Theor. **44**, 445308 (2011).

[47] H. Zhao, M. Bukov, M. Heyl, and R. Moessner, Adaptive Trotterization for time-dependent Hamiltonian quantum dynamics using piecewise conservation laws, Phys. Rev. Lett. **133**, 010603 (2024).

[48] J. Aftab, D. An, and K. Trivisa, Multi-product Hamiltonian simulation with explicit commutator scaling, arXiv:2403.08922.

[49] J. Geiser, Multi-product expansion with Suzuki's method: Generalization, Numer. Math.: Theory Methods Appl. **4**, 68 (2011).

[50] Y. Ouyang, D. R. White, and E. T. Campbell, Compilation by stochastic Hamiltonian sparsification, Quantum **4**, 235 (2020).

[51] S. Jin and X. Li, A partially random Trotter algorithm for quantum Hamiltonian simulations, Commun. Appl. Math. Comput. **7**, 442 (2025).

[52] M. Hagan and N. Wiebe, Composite quantum simulations, Quantum **7**, 1181 (2023).

[53] K. Nakaji, M. Bagherimehrab, and A. Aspuru-Guzik, High-order randomized compiler for Hamiltonian simulation, PRX Quantum **5**, 020330 (2024).

[54] O. Kiss, M. Grossi, and A. Roggero, Importance sampling for stochastic quantum simulations, Quantum **7**, 977 (2023).

[55] A. M. Childs, D. Maslov, Y. Nam, N. J. Ross, and Y. Su, Toward the first quantum simulation with quantum speedup, Proc. Natl. Acad. Sci. USA **115**, 9456 (2018).

[56] M. Kieferová, A. Scherer, and D. W. Berry, Simulating the dynamics of time-dependent Hamiltonians with a truncated Dyson series, Phys. Rev. A **99**, 042314 (2019).

[57] Y.-H. Chen, A. Kalev, and I. Hen, Quantum algorithm for time-dependent Hamiltonian simulation by permutation expansion, PRX Quantum **2**, 030342 (2021).

[58] D. An, D. Fang, and L. Lin, Time-dependent Hamiltonian simulation of highly oscillatory dynamics and superconvergence for Schrödinger equation, Quantum **6**, 690 (2022).

[59] D. Fang, D. Liu, and R. Sarkar, Time-dependent Hamiltonian simulation via Magnus expansion: Algorithm and superconvergence, Commun. Math. Phys. **406**, 128 (2025).

[60] A. D. Bandrauk and H. Lu, Exponential propagators (integrators) for the time-dependent Schrödinger equation, J. Theor. Comput. Chem. **12**, 1340001 (2013).

[61] G. Chen, M. Foroozandeh, C. Budd, and P. Singh, Quantum simulation of highly-oscillatory many-body Hamiltonians for near-term devices, arXiv:2312.08310.

[62] P. A. M. Casares, M. S. Zini, and J. M. Arrazola, Quantum simulation of time-dependent Hamiltonians via commutator-free quasi-Magnus operators, Quantum **8**, 1567 (2024).

[63] S. Blanes and P. C. Moan, Fourth- and sixth-order commutator-free Magnus integrators for linear and non-linear dynamical systems, Appl. Numer. Math. **56**, 1519 (2006).

[64] A. Alvermann and H. Fehske, High-order commutator-free exponential time-propagation of driven quantum systems, J. Comput. Phys. **230**, 5930 (2011).

[65] T. Barthel and Y. Zhang, Optimized Lie–Trotter–Suzuki decompositions for two and three non-commuting terms, Ann. Phys. **418**, 168165 (2020).

[66] J. Ostmeyer, Optimised Trotter decompositions for classical and quantum computing, J. Phys. A: Math. Theor. **56**, 285303 (2023).

[67] K. Mizuta, T. N. Ikeda, and K. Fujii, Explicit error bounds with commutator scaling for time-dependent product and multi-product formulas, arXiv:2410.14243.

[68] L. Zeng, J. Zhang, and M. Sarovar, Schedule path optimization for adiabatic quantum computing and optimization, J. Phys. A: Math. Theor. **49**, 165305 (2016).

[69] D. An and L. Lin, Quantum linear system solver based on time-optimal adiabatic quantum computing and quantum approximate optimization algorithm, ACM Trans. Quantum Comput. **3**, 1 (2022).

[70] V. M. Kendon, K. Nemoto, and W. J. Munro, Quantum analogue computing, Philos. Trans. R. Soc. A **368**, 3609 (2010).

[71] E. Forest and R. D. Ruth, Fourth-order symplectic integration, Physica D **43**, 105 (1990).

[72] S. Blanes, F. Casas, and J. Ros, Extrapolation of symplectic integrators, Celest. Mech. Dyn. Astron. **75**, 149 (1999).

[73] C.-F. Chen, H.-Y. Huang, R. Kueng, and J. A. Tropp, Concentration for random product formulas, PRX Quantum **2**, 040305 (2021).

[74] D. Fang, L. Lin, and Y. Tong, Time-marching based quantum solvers for time-dependent linear differential equations, Quantum **7**, 955 (2023).

[75] S. Garnerone, P. Zanardi, and D. A. Lidar, Adiabatic quantum algorithm for search engine ranking, Phys. Rev. Lett. **108**, 230506 (2012).